FACULDADE DE ENGENHARIA DA UNIVERSIDADE DO PORTO

FEUP

Autonomous paraglider for STRAPLEX

Mário Martins de Sousa

Mestrado Integrado em Engenharia Electrotécnica e de Computadores

Orientador: Sérgio Reis Cunha (PhD)

July 27, 2012

Resumo

STRAPLEX (*S*tratospheric Platform Experiment) é um projeto que oferece à comunidade científica uma nova forma de levar as suas experiências até à estratosfera. Dependendo da sua massa total, a plataforma é capaz de atingir 40 km de altitude, utilizando para isso um balão cheio de hélio. Após o rebentamento do balão devido à expansão do hélio num ambiente de baixa pressão, a plataforma inicia a descida auxiliada por um pára-quedas circular. Isto torna impossível definir o local de aterragem, que dependerá exclusivamente da direcção e velocidade do vento. Esta dissertação propõe uma nova abordagem que possibilita o controlo do STRAPLEX durante a descida.

A introdução de um parapente autónomo na plataforma possibilita que locais de aterragem indesejados, tais como áreas populadas e corpos de água possam ser evitados. Isto constitui uma melhoria de segurança e uma diminuição no tempo de resgate. Uma cápsula especialmente desenvolvida chamada de *D*rone incorpora os servo-atuadores e os sistemas de navegação e orientação. Esta cápsula é responsável pelo controlo da asa tanto em modo manual como em piloto automático. O computador a bordo da cápsula principal, destinado essencialmente ao registo de informação e previsão do local de aterragem, é substituido por um módulo desenvolvido no âmbito deste trabalho. Este dispositivo é capaz de descodificar tons DTMF, desmodulação 5DPSK, modulação GFSK para enviar telemetria no canal de áudio do ATV e interagir com o transceptor de GFSK. Desta forma, para além de substituir o computador, substitui também outros equipamentos a bordo eliminando a assim a massa dos mesmos e das respectivas baterias. O sistema de *c*utdown foi também sujeito a modificações para melhorar a sua fiabilidade. Um protocolo de comunicação é implementado a fim de permitir a partilha de informação entre os diferentes módulos que constituem plataforma.

Os voos realizados demonstraram a capacidade do piloto automático manobrar a plataforma a fim de se aproximar e seguir linhas definidas por conjuntos de pontos. Deste trabalho conclui-se que este método é passível de ser posto em prática neste tipo de plataformas.

Abstract

STRAPLEX stands for Stratospheric Platform Experiment and offers the scientific community a new way of taking their experiments to the stratosphere. Using an helium-filled balloon, this platform can reach up to 40 km in altitude depending on the total mass. After the balloon burst due to helium expansion in a low pressure environment, it starts to fall aided by a round parachute. This makes it impossible to control the landing site, depending only on the wind speed and direction. This dissertation proposes a new approach that will make STRAPLEX steerable during the descending phase of the flight.

This work introduces an autonomous paraglider into the platform. Therefore, undesired landing spots such as populated areas and water bodies can be avoided. This implementation contributes to safety improvement and a decrease in the rescue time. A special capsule called *D*rone incorporates the actuators, navigation and guidance systems. This capsule is responsible by the control of the canopy either with in manual mode or in autopilot mode. The on board computer in the main capsule was replaced by a module developed in this work. This device is capable of decode DTMF tones, a 5DPSK demodulation, GFSK modulation to send telemetry over the ATV audio channel and interact with a GFSK transceiver. Thus, it replaces a few equipments on board cutting out mass. The cutdown system was also subject to modifications to increase its reliability. A communication protocol was implemented to allow the exchange of information between different modules that compose the platform.

The flights performed showed the ability of the autopilot to maneuver the platform in order to approach and follow lines defined by sets of points. This work concludes that this method may be applied in this kind of platforms.

Agradecimentos

Exprimo os meus mais sinceros agradecimentos ao meu orientador, o Prof. Sérgio Reis Cunha, não só pela sua dedicação, incentivo e disponibilidade, mas também pelo seu entusiasmo contagiante. Agradeço aos meus colegas e amigos Ricardo Dias e João Pinho pelas ideias que deram na elaboração deste documento.

Estou também grato à minha família que sempre me apoiou e me permitiu que trabalhasse em horários, por vezes, pouco convencionais. Pela paciência e compreensão durante este ano, um especial agradecimento à minha namorada, Joana.

Mário Martins de Sousa

"Design is an iterative process. The necessary number of iterations is one more than the number you have currently done.
This is true at any point in time."

Akin's Laws of Spacecraft Design

Contents

List of Figures

List of Tables

Abbreviations and Symbols

AHRS	*Attitude and Heading Reference System*
APRS	*Automatic Packet Reporting System*
ASK	*Amplitude Shift Keying*
ATV	*Amateur TeleVision*
CoCom	*Coordinating Committee for Multilateral Export Controls*
CPU	*Central Processing Unit*
FEC	*Forward Error Correction*
FSK	*Frequency Shift Keying*
GFSK	*Gaussian Frequency Shift Keying*
GPS	*Global Positioning System*
I2C	*Inter-Integrated Circuit bus*
IMU	*Inertial Measurement Unit*
ISM	*Industrial Scientific and Medical*
OEM	*Original Equipment Manufacturer*
OOK	*On-Off Keying*
PCB	*Printed Circuit Board*
PSK	*Phase Shift Keying*
RF	*Radio Frequency*
SD	*Secure Digital*
SMPS	*Switched-Mode Power Supply*
SPI	*Serial Peripheral Interface*
STRAPLEX	*STRAtospheric PLataform EXperiment*
TTL	*Transistor-Transistor Logic*
UHF	*Ultra High Frequency*
USART	*Universal Synchronous Asynchronous Receiver Transmitter*
USB	*Universal Serial Bus*
VHF	*Very High Frequency*
VNA	*Vectorial Network Analyzer*

Chapter 1

Introduction

1.1 Objectives

Paragliders are lightweight with no rigid structures glider aircrafts. They are used in a recreational or competitive adventure sport called paragliding. A paraglider is composed by a ram-air wing that uses lines to suspend a harness where the pilot sits. The wing, also called canopy, is made of thin fabric structure organized in cells with a frontal air intake which allows the wind to inflate it. After inflated, the canopy has an airfoil shape. Since it is a non rigid air-inflated form it is called parafoil. The aim of this thesis is to explore the controllability problem of a paraglider launched at 40 kilometers in altitude intended to follow a given path till the landing. This paraglider suspends not a pilot but an high altitude platform called STRAPLEX that rose with an helium-filled balloon.

The control dynamics involved in an aviation system are very challenging. The amount of variables and the non static environment make it difficult to analyze. The pendulum effect, the non rigid wing structure and wind compensation are further issues the control algorithm must deal with. On the other hand a strong communication protocol must be implemented in order to exchange information between the systems that compose STRAPLEX and the ground station. The results from this study come from a strong theoretical background, combined with the physical implementation of the whole system.

1.2 Motivation

Flying has been one of the mankind's dream since the Da Vinci's flying machine, the Montgolfier brothers' hot air balloon and the Wright brothers' plane. STRAPLEX allows students to fly their experiments in the stratosphere while developing engineering skills. The stratosphere is the ideal place for experiments that need to be exposed to extreme conditions such as radiation, low atmospheric pressure and high temperature amplitudes. The author has been participating in this project for five years and during this time some missions landed in locations of difficult recovering. For

example, one of the flights landed in a quarry in Spain and required the Spanish authorities intervention in the rescue operation. The will of avoiding this kind of situations and the author's fascination with the aviation led the dissertation to this topic. A controllable descending phase makes it possible to land in a predetermined location reducing the rescue operation time and the inherent risks to the landing that although being low, exist.

1.3 Thesis structure

This thesis is composed by six chapters. After this one with introductory purposes, it will be presented the problem that is in the origin of this work, the approach to solve it, the state of the art and the current state of the STRAPLEX project. It will be an overview of the whole work developed. The third chapter aims to show the modules on board and how they interact with each other with a detailed description of mechanical, hardware and software features. The ground station systems are explained in the forth chapter. The fifth chapter includes a description of ground and flight tests executed whereas the sixth presents the conclusions and future work.

1.4 Website

A website was created at apstraplex.pt.vu to provide the reader more details about this study. It contains a short description and objectives of the work developed. Weekly reports can be downloaded from the section with the same name. In the area "Gallery" it is possible to watch photos related to the systems development as well as videos of some tests and flights. A briefly information about the author is also available in the section "About Me".

Chapter 2

Overview

This chapter aims to provide the reader a background of the project STRAPLEX. It will explain how it is constituted and its history. Then, a systematic overview of the problem and the approach proposed here to solve it. This chapter ends with the developments made in addressed area by other authors and the technology available at this time.

2.1 STRAPLEX, The project

The STRAPLEX project is a platform that offers the scientific community the possibility to send their experiments to the stratosphere using helium-filled balloons. This programme is a partnership between the Faculty of Engineering of the University of Porto and the European Space Agency (ESA). It consists on a main capsule that carries both the experiment and the control system. A secondary capsule attached to the main one accommodates a transponder used in aviation. This platform climbs to the stratosphere using a balloon filled with helium. Depending on its total mass, STRAPLEX can fly up to 40 kilometers in altitude where the platform is exposed to an environment very similar to space. At this flight level, due to the low atmospheric pressure, the balloon is approximately six times bigger and the latex of which it is made reaches its rupture point. After the balloon bursts, the platform descends aided by a round parachute. The system on-board logs the flight parameters, calculates the estimated landing site and manages all the communications. A fixed ground station tracks down the platform during all flight, receiving the current position and a live ATV feed. In the meanwhile, a mobile station heads towards the estimated landing region in order to rescue the capsule as soon as it lands. The airfield of Évora is the chosen site for the launches due to the low urbanization and flat terrain found in the Alentejo region. The good relationship with the airfield administration and the excellent support they always provided is also an added value to this project.

This project started by a student initiative in 2005 and some months later it was flying over the skies of Évora for the first of five qualification flights. These flights took place in order to develop

and validate the several systems of the platform. In October of 2006, the first student campaign took place at Évora airfield with experiments from two teams. A team from Netherlands measured the gravity acceleration during the flight. The experiment from Spain consisted in the evaluation of the performance of specific semiconductors exposed to the solar radiation. Due to a southwest wind, the platform flew 170 km landing near Mérida, Spain. In September of 2008, teams from three countries joined for the second flight with experiments on board. Shortly after the launch, the VHF and UHF communication failed probably due to a damaged antenna. This prevented a good tracking of the platform, since the only device reporting its position was the transponder which is only visible by an aviation secondary radar. The platform rose to an altitude of 30 km in about two hours drifting in a light breeze. Then it started the descent landing 45 minutes later in the Alqueva dam. The communications failure combined with the landing location, forced the use of a search aircraft to help in the rescue process. At the time of the campaign, although the Alqueva dam wasn't at full capacity, several existing tracks were already submerged, making the landing place even more remote. The closer access to that place was in the opposite shore. Three elements of the rescue group had to swim and tow the platform to the shore closer to the road. This splashdown caused a 24 hour delay in the recovery. Besides that, all the experiments on board were a success.

2.2 The problem

During the descending stage, due to the characteristics of the circular parachute, there wasn't any kind of control mechanism. The landing site depended only on the wind speed and direction. Places like populated areas, roads, private properties and water bodies were, therefore, unavoidable. This could cause severe damages to the platform and pedestrians or could even originate the theft of the equipment. The European Space Agency forces to calculate the risks inherent to the the launches. The landing, due to the location uncertainty, is the bigger risk since the chances of a collision with an aircraft are small after the introduction of the transponder. Moreover the platform often lands in Spain, sometimes 150 kilometers away from the launch site. The time spent in the rescue operation makes it impossible to reuse the capsule for another launch in the same day. These issues are an important factor on the mission success.

2.3 The approach

As stated above, STRAPLEX cannot control the descending path, being that the motivation of this thesis. The ability to maneuver the platform opens the door to avoid undesirable landing spots, longer flights at high altitude and faster rescue operations. To the actual parachute was added a parafoil which provides the system with two degrees of freedom. Thus, the descent has two stages. In the first stage, a conventional parachute decreases the vertical speed until the platform reaches the more stable air masses at medium altitudes. At this point, the wing is deployed and the platform is now steerable. A new capsule called Drone was added with the purpose of controlling the canopy. Actuating on a set of four lines, Drone is able to define direction and sink rate.

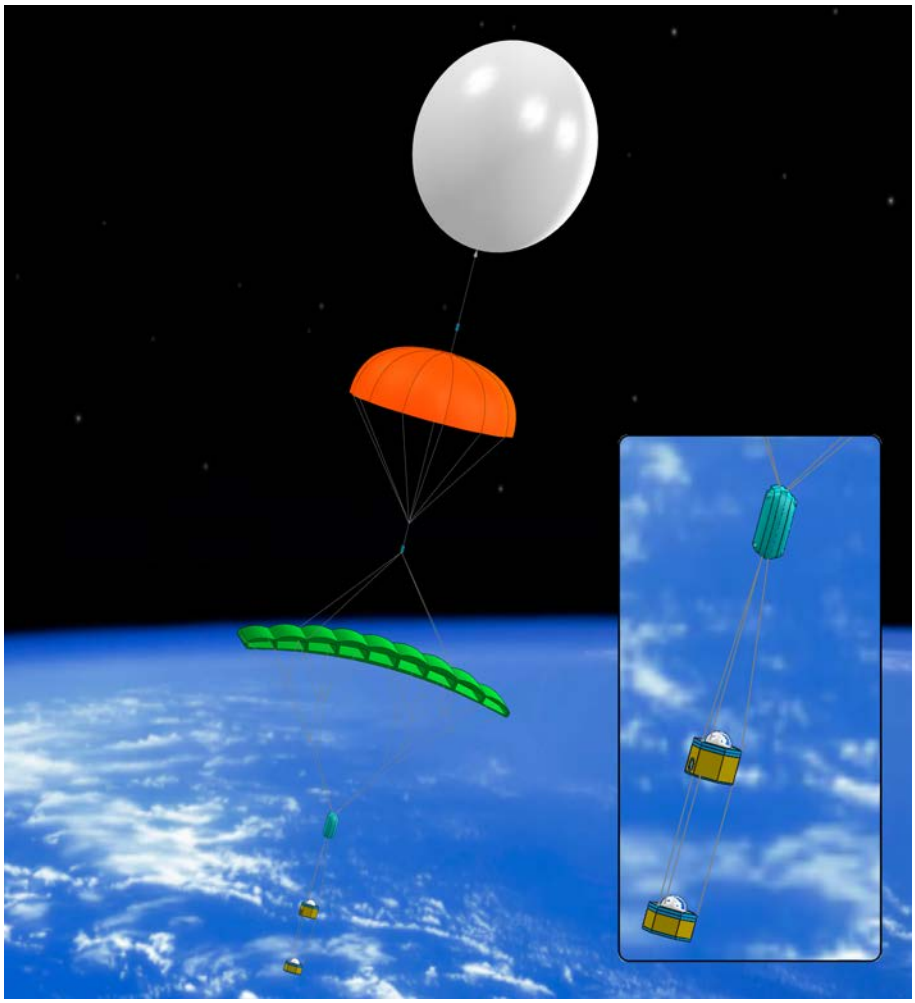

Figure 2.1: STRAPLEX

However the lack of a thrust source does not allow navigation against the wind, the system takes advantage from the collected data to choose the best way to land on the desired spot. A manual mode and four types of autonomous modes are possible. This allows the user to manually control the platform if needed. Otherwise, the autopilot is able to perform tasks such as follow a given heading or fly over a line. The system is fully configurable during the flight.

2.4 State of the Art

The interest on controlling autonomously the ram-air parachutes is not new. These systems have several applications such as delivering loads in remote areas, military surveillance and landing systems for maned vehicles, probes and rocket recovery. This concept was explored by NASA at Dryden Research Centre between 1991 and 1996 [1] [2]. The Spacecraft Autoland Project was initiated to evaluate the possibility of using autonomous ram-air parachutes for the final stage of entry from space.

The development and refining of this project was divided into three phases which carried out dozens of test flights. The goal of this study was demonstrate the feasibility of autonomous navigation and soft landing at a given landing site after the deployment at 3000 m altitude and an offset of 1.6 Km. The desired precision was a 400 m radius circle centered at the landing site. The capsule had a biconic shape 1.2 m long where the navigation, guidance and control systems were placed. Two large commercial servos provided 380 kg.cm of force to actuate the lines. The control signal of this devices could be feed either from the autonomous system or directly from a compatible uplink receiver whenever in manual control mode. The uplink was possible using a radio controlled model transmitter boosted to 15 W operating in a government reserved frequency. Different sizes of commercially available parafoils were used to achieve different wing loadings. The first phase was intended to demonstrate the feasibility in applying a navigation system to maneuver a canopy. The mass of the vehicle in this phase was about 68 kg and included batteries, an on board computer, altimeter, magnetometer and GPS. It flown under a 26.8 m^2 ram-air parafoil which yield to a wing loading of 2.4 Kg/m^2, the usual for a parachuting student. This light wing load provided an extra safety measure for the first phase flights.

Ground tests were conducted to validate the control algorithm and the overall working condition of the capsule. These tests included the vehicle mounted in the top of a van with the control lines hanging in front of the driver who steered accordingly to them. The implemented algorithm only tracks heading and so it wasn't able to follow a given profile due to the non controlled cross track error. After the successful ground tests, the vehicle was launched several times from an airplane at altitudes up to 3000 m where the validation of each system was performed.

Instead of deriving a theoretical model of the flight dynamics, the post flight data was used to identify the simplest model that would consider the essential components. In order to establish the model, a set of step and impulse in flight maneuvers were conducted to calculate the control gain, natural frequency and damping. After averaging several similar maneuvers, the transfer function was estimated as being 0.6 for the gain, 2.5 rad/s for the natural frequency and a damping of 0.3. The control algorithm used a magnetometer and a gyroscope as feedback input. These signals are applied to a complementary filter which estimates the yaw rate. For yaw rates higher than 0.2 rad/s, the magnetometer signal became unreliable and the filter was replaced with a simple integration of the gyroscope. This work concluded that the implemented algorithms worked well up to 24 km/h winds. With winds approaching and exceeding the flight speed of 32 km/h the control algorithms failed. The average landing error for the demonstration flights was about 120 m. Data for post flight wind estimates was gathered performing a three-circle maneuver. In null wind conditions, the path described by the vehicle would superimpose. In the presence of wind, the circles progressively shift their center. This method assumes a constant wind velocity at the different altitudes where the circles were executed. Before this flight, a set of foil-covered streamers were dropped from the launch aircraft and tracked by a radar. The difference between the radar and GPS measurements showed a difference of less than 0.6 m/s. Although being reasonably accurate, this wind estimation method is not practical for real-time applications.

For the phase 2, an airspeed sensor was installed to overcome the problems with stronger

winds. Ground tests were performed to calibrate the true airspeed of this sensor. To achieve this, the vehicle was mounted on the top of a van and the airspeed compared to the GPS ground speed. During this stage a delay in the GPS speed reading was identified, ranging from 2.0 to 2.3 seconds. In this phase, a 8.2 m^2 parafoil it was employed along with a ballasted vehicle up to 79 kg which yields to a wing loading of 9.8 m^2. This allows to investigate the scalability to the typical wing loading of a full-scale spacecraft. Another issue addressed in the second phase was the flaring system. Flare, in parafoil terminology, means applying full brakes for short time moments before the touchdown. This maneuver raises the drag of the wing, slowing down the vehicle for a soft landing. If applied too early, the reduced speed causes a sudden loss of lift and, therefore, a high vertical speed. The brake lines could be pulled by high torque servo-motors but their usage just for a short period of time in a full flight would not worth the added mass they would represent. The approach used by the authors consisted in attaching the brakes directly to the rear of the vehicle. When the flare is required, a pin that holds the capsule in the horizontal position is pulled off, leading to the descent the rear part of the vehicle and consequent pull of the brakes. The tests showed that a flare initiated at 8 meters above the ground effectively reduced the sink rate from 3 m/s to 0.6 m/s.

The third phase of this project intended to evaluate the *P*recision Guided Airdrop Software (PGAS) system. Since this phase was used to develop precision offset cargo delivery to the Army, there isn't more information available.

A paraglider dynamics model is presented in [5]. This work also simulates a control algorithm based on the model achieved. The work developed by Toglia et al. [3] shows an algorithm that is able to follow a polygonal path with error converging to zero within 50 seconds after each change in the flight direction. This algorithm considers a 6 degree of freedom model and accounts for several factors such as weight and aerodynamic forces. The author derived a complete model of the paraglider dynamics based on the physical concepts to which it is subjected. For comparison purposes, a simplified model has been developed by neglecting effects with less weight at near steady-state condition. The simulations showed that both models have a comparable convergence rate and tracking accuracy.

A final approach strategy algorithm that corrects the bias introduced by the wind is presented by Sledgers et al. in [4]. This work proposes a guidance strategy divided in seven distinct phases with special incidence in the control algorithm for the sixth one. In the first one, after the canopy opening, the control is halted till stabilization is achieved. After that, the following phase takes the paraglider to a given area. The third phase executes a spiral maneuver in this specific area and winds are estimated. When the switching altitude is reached, the algorithm starts phase four and five which are composed by exiting the spiral and fly parallel to the final approach respectively. Phase five composes the final turn to the approach glide slope. The flight ends with the final approach landing into the wind. In the first five phases, the algorithm simply heads to the next tracking point. However, in the last two phases, the optimum trajectory is continuously computed to take into account unexpected wind changes.

Kaminer et al. developed and simulated a control algorithm in several maneuvers in [6]. A

similar work was developed for a powered paraglider in [7]. The control of a UAV based on a PID control loop feedback mechanism is developed in [10]. This work uses off-the-shelf modules with interesting performance.

On the industry side, *Atair Aerospace* is one of the companies developing solutions using autonomous paragliders. Atair aerospace developed the *O*nyx product family which is an autonomous precision airdrop system in compliance with the U. S. Army's Joint Precision Airdrop System (JPADS). The JPADS program specifies the characteristics of airdrop systems that use GPS and parachutes steered by an on board computer to deliver loads on a given landing point. It merges the *U. S. Army's Precision and Extended Glide Airdrop System* (PEGASYS) and the *Air Force's Precision Airdrop System* (PADS) program. PEGASYS comprises steerable airdrop systems designed for several types of load. In the other hand, PADS consists on a software that predicts the optimal point to drop non-steerable parachute systems taking into account atmospheric variables such as wind, air pressure and temperature. Currently, there are two products available which differ only in load capabilities. A light version handles loads from 4.5 kg to 68 kg whereas a heavier one is able to deliver loads from 113 kg up to 318 kg. These systems employ adaptive control capable of correcting load changes, asymmetrical load and damage induced in flight. Since several systems could be deployed at once, collision avoidance algorithms are also used, enabling even formation flying towards one or multiple targets. These features are highly relevant in hostile areas such as an war zone. The devices may be tracked in real time by a software which displays their position overlaid on a 2D and 3D maps.

*A*tair also developed a product family of powered autonomous paragliders for surveillance and reconnaissance missions. With a maximum altitude of 15 000 m, they are capable to carry up to 90 kg of equipment in 48 hour missions. These devices can take off in a space of 45 m or be air-deployed from cargo aircrafts such as the lockheed C-130. *Airborne Systems* is another company offering guided precision aerial delivery systems. It has four different products to payloads that range from 45 kg to 4500 kg. The device with higher load capacity has a maximum glide of 3.75:1 and a ceiling of 7620 m. New products are being developed for heavier payloads [8]. This products fulfill the JPADS requirements and except in load capacity, they are very similar to the *Atair Aerospace* solutions. Both companies state that their products land with a precision of 150 m. From the guidance algorithms point of view, most of the development in this area is circumscript to the military and spacial industry and therefore not public. However some developments in this area are sometimes published such as in a compact mobile aerial delivery system with high accuracy proposed by [9] and the article [12] that describes the modeling stage and control system.

As stated above, the automation of paragliders is not new, however its use on high altitude platforms is. In that perspective there is no background work that could be used for this study. Most of the used hardware can be found in the aviation industry. The inertial measurement unit (IMU) is a device used in aircrafts to report velocity, orientation and gravitational forces. It is used not only in navigation but also to stabilize the airplane and it is composed by accelerometers, gyroscopes and magnetometers. The aviation industry offers a wide range of options with different prices. The most expensive units have a moderate range in what concerns to the maximum angular velocity

and what distinguishes them from the cheaper ones is the low bias and low random walk. Only devices with this characteristics can have good performance in dead reckoning systems. However, these products are designed to be robust and flexible for different environments. The weight, the power requirements and the prohibiting prices of aviation units force the use of hobbyist directed IMU's. These units usually operate at 3.3 V or 5 V and weight a few grams. Attitude and heading reference systems (AHRS), which differ from IMU's by giving the processed sensor outputs in the form of pitch, roll and yaw, are also available.

Positioning systems are essential for this kind of applications. The GPS receivers have been developed in the sense of miniaturize and reduce the power requirements. Manufacturers such as uBlox and Trimble have product families for different types of applications. The different modules are a trade off among size, active antenna support, voltage range, update rate, number of communication ports and cost. The communication ports are available as RS232, USB, SPI or I2C interfaces. Another parameter used for module performance comparison is the sensitivity and the time to first fix in different conditions. Modern devices have an update rate as high as 5Hz and may be aided with external data containing rough position coordinates. This improves substantially the time to first fix in a cold start. All publicly available devices comply with the CoCom restrictions which state that a device traveling faster than 1900 km/h at an altitude higher than 18000 m should disable tracking to avoid being used in ballistic applications. This limits should be applied as a logic "and". However, some manufacturers disable tracking when one of the two limits is reached which is an issue to high altitude platforms. From previous experiments, it is known that uBlox implements correctly these limits.

Several solutions for communication systems are commercially available. From the conventional radio-controlled models transmitters and receivers to the latest digital modulation transceivers, there are a wide range of options for all purposes. In spite of the radio-controlled models like systems being very reliable and easy to use, they are suitable only for manual controlled applications. Whenever custom data is supposed to be exchanged between two or more devices, digital transceivers are the best option. These devices vary in modulation used, power transmitted and processing options. Low cost devices usually use simple modulations such as on-off keying (OOK) or amplitude shift keying (ASK) without packet handling capabilities. The transmitted power is around 13 dBmW and the receivers have low sensitivity restraining the communications to a few dozens of meters. Better transceivers use more robust modulations such as frequency shift keying (FSK) or phase shift keying (PSK) and provide adjustable operation frequency. Automatic packet handling is also an important feature, since it reduces the development effort and the processing requirements of the microcontroller. A maximum output power of 20 dBmW along with enhanced sensitivity allow communications that may extend for a few kilometers in line of sight (LOS). Spread spectrum techniques and multi channel capabilities are found in the high end products.

Chapter 3

Control System

This chapter is split into three sub chapters. In the first sub chapter, the interaction among the different modules and the control chain is described. The second one, called Drone, is further divided in four sections. The first section details the canopy operation and mechanical aspects of the controller. The following one describes the modules built and how they interact. The software section details the routines executed in the microcontroller while the operating modes explains the platform operation philosophy. The last section analyzes with more detail the control algorithm. The subsystems present on the main capsule are explained in the third sub chapter. These include the communications channels and the cutdown device.

3.1 Communications architecture

The communication between the platform and the base station must have redundant channels. This avoids a total blackout if one of the systems fail. However, each additional channel comes at the cost of space, mass and energy. Thus, all communication opportunities present in the equipment already installed are exploited.

Figure 3.1 shows an overview on the communication network. The base station is able to send information to the the platform through three different means. The more flexible communication method, which allows the communications directly with the main capsule, with Drone and with the cutdown systems, comprises on using a GFSK transceiver similar to the ones installed on the platform. However, the output power of this device has been amplified from 20 dBmW to 33 dBmW and the monopole radiator element replaced by a yagi antenna with a gain of 13 dB. Still, this equipment may be unable to establish a solid connection at longer distances. If this is the case, another uplink channel can be employed. A 5DPSK modulation is injected in the audio of a VHF amateur-radio transceiver capable of delivering up to 47 dBmW, which allows the transmission of a basic set of commands. This channel is received only in the main capsule which relays the commands though the GFSK transceiver to the correct destination if needed. In

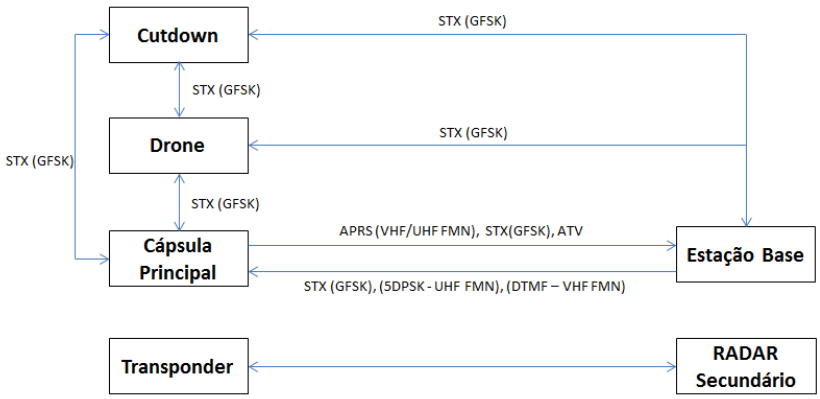

Figure 3.1: Information flow

the worst-case scenario an even more robust method can be used. Sixteen different DTMF tones may be transmitted on the UHF band, enabling the execution of sixteen different actions. Most amateur-radio transceivers have this feature built-in.

The base station receives data from four different sources. The GFSK transceiver already described is able to receive not only the packets directed to its address, but also intercept the communications between the modules on board of the platform. The position coordinates and elementary information is received in both VHF and UHF APRS channels. Taking advantage from the unused ATV audio channel, a GFSK modulation is employed to broadcast high baud rate telemetry data.

An aviation transponder is installed in the platform to increase the safety levels. With this device, the platform is visible to the air traffic controller through a secondary radar as well as to the other nearby aircrafts equipped with the traffic collision avoidance system (TCAS).

3.2 Drone

The need to control the canopy led to the construction of another capsule beside the existing ones. The Drone must be able to actuate the lines that drive the paraglider and, in the first stage, stabilize it. After this, the controller will maneuver the wing in order to follow the commands given by the navigation loop.

3.2.1 Mechanical structure

A parafoil is made of a thin fabric divided in small sections called cells. Intakes in the leading edge of the wing allow the inflation of the cells giving it the characteristic shape. The canopy for this application was adapted from a common recreational power kite. This kind of wings are intended to provide enough force to lift the user with small wind gusts and therefore its shape shows a bigger wind resistance than, for example, a manned paragliding wing. However, due to

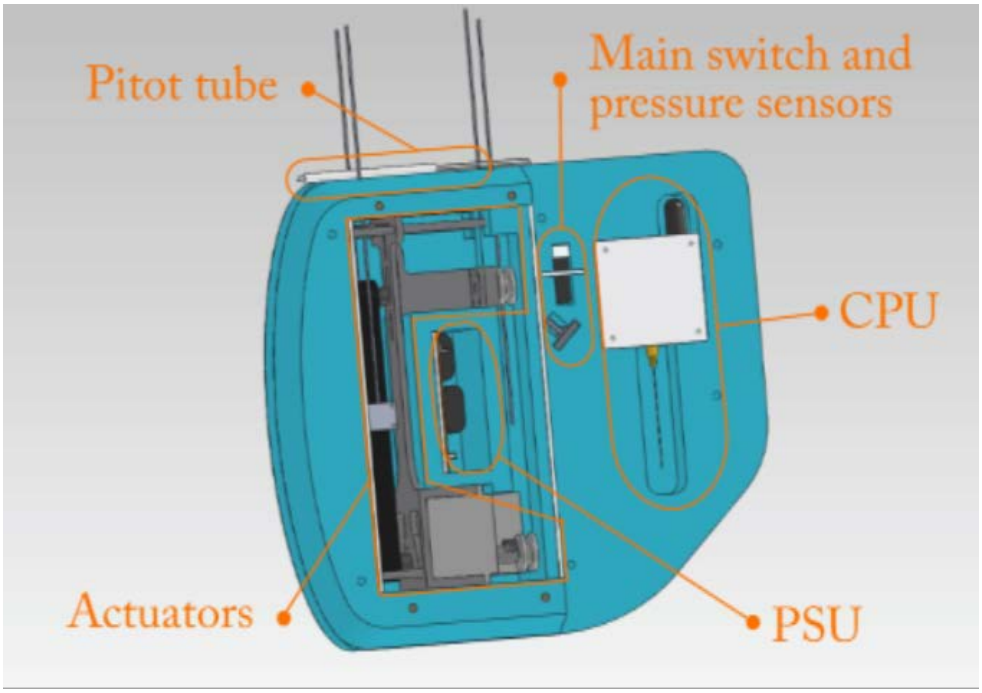

Figure 3.2: Drone 3D Model

the difficulty of finding an appropriate paragliding wing for the mass of the platform, a power kite of three square meter was chosen and called paraglider indistinctly. The expected wing loading with the full platform is 2.3 kg/m^2 which is the typical value for a parachutist. This canopy is actuated by four lines which combination causes a different flight behavior. Two main cables, which also provide the lift force, are used in a differential mode to deflect the wing. The deflection will induce a change in the flight direction with minor impact on its efficiency. The breaks are another two strings which can be used independently to make an yaw movement or combined to decrease the horizontal speed and increase the sink rate. Since the canopy has no rigid structure, it can collapse due to several factors. The angle of attack is a key point in what concerns to maintain the wing inflated. A too high angle of attack prevents the air from flowing to the cells, decreasing their pressure. A too negative angle of attack may induce forces in the upper layer of fabric making the wing deflate. Wide swings may also produce the same effect. If at any time, one of the control lines get loose, the wing can lose its shape and collapse. Usually, this events are self-recoverable at the cost of losing altitude. However, in some cases, the canopy gets entangled in the lines making it impossible to recover.

The current mass of the platform is about 6 kg and therefore the Drone (Figure 3.2) must support at least 60 N of tractive force along its structure. Furthermore, during the descent, it is possible to experience some turbulence that may create additional mechanical stress. The region of the structure that suffers these forces is built from a single piece of aluminum with a shape similar to a violin which is the mainframe for all other parts (Figure 3.3). Using Solidworks, this part was designed with small walls where the three servo-motors fit. Providing an anti torque

Figure 3.3: Aluminium structure

force, they relieve the forces applied to the four M2 screws that hold each servo-motor in place. The central servo-motor, which is also the main one, is placed upside down and the spare space is used to fasten a bearing to the mainframe. In the other tip of this piece, there is room to fix a sliding belt tensioner and two line guides. A boom reinforced with a perpendicular rib connects the two regions of this part. In the corners of each face there is an aluminum pipe that holds one of the two PVC rims that give to the whole structure a parallelepiped shape. All ninety degree angles are softened with fillets to enhance the resistance while maintaining the low weight provided by the aluminium. One of the biggest challenges of the controller is the interface between the servo-motors and the lines. Thus, special care was taken in its design process. Three systems of one belt and two pulleys are used on the mechanism to prevent the lines get entangled. The main belt is an HTD timing belt which provides enough strength to suspend the platform while the brake belts are made of Dyneema. Each pulley is fixed to its own shaft with a screw. Clamped to the main belt are two segments of steel cable while each brake system has only one. These four segments will then connect to the canopy lines outside the Drone capsule. Steel was used instead of the Dyneema line because its hardness makes it difficult to tie itself when it isn't stretched. The three servo-motors are located on the side of the two pulley system that holds all the tractive force caused by the platform mass. This allows the belt teeth to be firmly coherent with the main pulley in order to avoid skidding.

The clamping system for the main cables was also designed in Solidworks and then machined in a homemade computer numerical control (CNC) machine. Composed by a spindler that can slide in three orthogonal directions, this machine is capable of reproducing a 3D model in soft

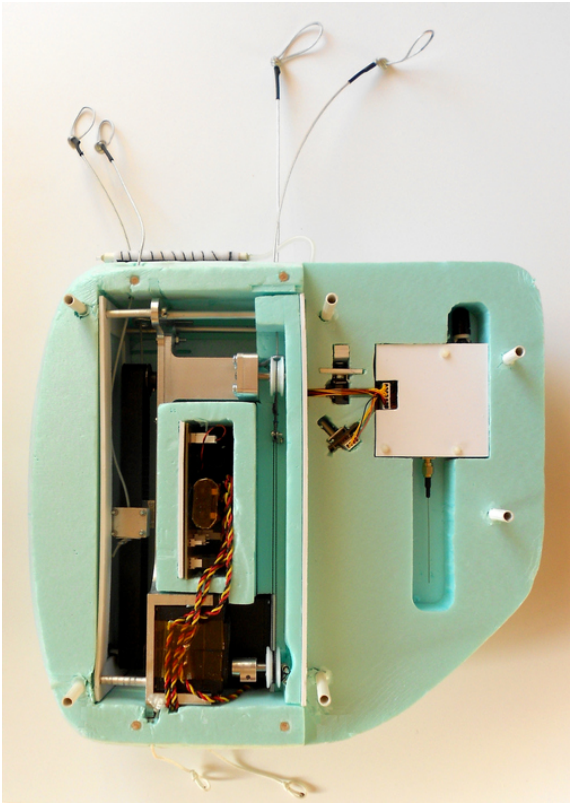

Figure 3.4: Drone open

materials. These clamps are made of a piece that squeezes the belt against a counter-mold of its teeth. Reinforcing the two nylon pieces there is a pair of steel sheets. Since weight is a big concern in this application, only the two main pulleys are made of steel. The other four are PVC pulleys with bearings that were adapted to be coherent with the respective shaft. The adaptation nylon part was machined in a lathe. The upper pulleys are attached to a piece that slides along the mainframe and allows an adjustable belt tension. This piece is held into place with a pair of screws. After assembling, the Drone weights about 1940 grams with the aluminium and steel parts along with the batteries being the major contributors.

In some STRAPLEX flights it was observed that, while climbing, the main capsule describes a slow rotation movement. On the other hand, changes in the wind direction may induce the same movement on the wing. These situations could twist the paraglider lines making them inoperative. Thus, two measures were taken. The line that links the Drone to the main capsule will allow it to fully rotate without twisting the line itself and the Drone will have an aerodynamic shape with a tail that will allow it to face the wind just like the canopy. Another design restriction is related to the distance between the main lines when they leave the control structure. As this distance increases, instead of deflecting the wing, the line will just apply a momentum to the structure. Therefore, to avoid this, a slim shape was preferred. However, with the lines so close, the wing has the tendency to arch its shape. This reduces the performance, decreasing the glide ratio. Thus,

a stabilization bar was installed about half a meter above the Drone. This serves two purposes: decrease the arch of the wing and insert an anti twist force. Although the stabilization bar solution could be replaced by increasing the length of the lines, tests shown that the extra length reduces the system controllability.

In order to maintain the internal temperature and dissipate the landing impact, Styrofoam is used as cover material. This light polystyrene foam has proved to be very effective on STRAPLEX capsules. The tail section is used for housing the electronics while the batteries are assembled on the main aluminium body for a correct mass distribution. A three-dimensional model of the Drone was made in Solidworks (Figure 3.2) taking into account aspects such as aerodynamics, impact robustness, center of mass and parts disposition to avoid the problems that metal can produce in the vicinities of the antennas. The model was later used to create the wood molds on the homemade CNC machine. Each Styrofoam layer is cut using a hot wire and the respective wood mold. The rounded shape of the two lateral layers is an exception to this method and needed to be machined. Some interior profiles need to be cut with the help of a sharp knife. To reinforce the capsule, the layers are glued along with several pipes screwed on each side. Only the left front and rear layers are not glued to allow access to the devices. Enclosed in the styrofoam there is a power switch that can be toggled inserting a stick in a slot and gently applying some pressure. This solution allows an easy access from the exterior and robustness against shocks. The lines that hold the remaining platform are tied to two holes in the bottom of the mainframe. Appropriate knots were used in the line junctions to ensure reliability while being easy to remove. The junctions are made of a bowline knot followed with a figure-eight knot on the tips to prevent sliding.

3.2.2 Hardware

Drone, as a separate but integrated system, must be able to power itself and execute control and communication functions. Therefore, a pair of lithium 6V non-rechargeable batteries will supply the servo-motors while another one is reserved to the CPU. The lithium non-rechargeable batteries are preferred to the rechargeable ones due to the higher power density and reliability. The specific model used in STRAPLEX is the 2CR5 from Ansmann which has a total capacity of 1400 mAh. The CPU draws an average current of 150 mA while the total estimated average current for the servo-motors is around 800 mA. This allows more than nine hours of CPU operation whereas the servo batteries last up to three hours and a half. These batteries are attached to a printed circuit board (PCB) called power supply unit (PSU) that also includes temperature and power monitoring devices. The supply voltage for the servo-actuators ranges from 4.8 V to 6 V so they can be powered directly from the batteries. On the other hand, the processing unit of the Drone needs a low noise 3.3 V power supply. With this purpose in mind, a switched-mode power supply (SMPS) followed by a 3.3 V low dropout regulator scheme was implemented. Since the regulator has a dropout voltage of 0.25 V at the maximum current expected, the SMPS biasing network was calculated to step down the voltage from 6 V to 3.85 V, which give a margin of error for component tolerances. The implemented method provides a good conversion efficiency combined with a low noise output voltage.

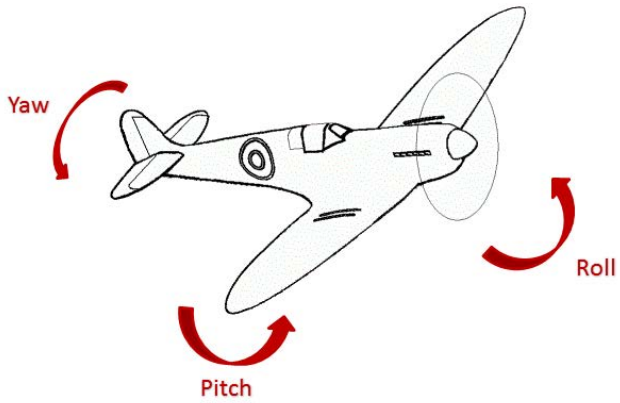

Figure 3.5: Attitude of a plane

As already explained, the PSU is located near the main aluminium part due to the influence of its weight on the center of mass. Although being on the mainframe, the PSU is isolated inside a styrofoam ring to protect it from low temperatures that could damage the batteries. The core of the Drone is a MSP430 microcontroller that joins the processing capacity with the low power requirements. It is installed on the CPU PCB that can be found in the styrofoam tail. One of its functions is to gather attitude and position data which is essential for an accurate navigation. To achieve that, Drone uses an attitude and heading reference system (AHRS) along with a GPS receiver while a pitot tube provides the airspeed. The AHRS, composed by a 3-axis accelerometer, magnetometer and gyro, uses a Kalman filter to give the processed pitch, roll and yaw angles at a rate of 20 measurements per second. Figure 3.5 exemplifies the application of these angles on a plane. The null angle state is defined by the aircraft in a upward position facing north with the wings parallel to the ground. Increasing the pitch angle means raise the nose of the plane whereas a positive roll is equivalent to a right turn. Yaw angle increments in a clockwise rotation. The module is also able to give this information in the form of a quaternion which eliminates the singularity on Euler output at $+\frac{\pi}{2}$ and $-\frac{\pi}{2}$ pitch angles. However, wide pitch angles are not expected, Euler output is used instead.

For position and velocity information a uBlox GPS receiver is used. The particular model NEO-6Q was chosen due to the small form factor, suitable voltage supply, low cost and wide operating temperature range. A quadrifilar helix active antenna from Sarantel is employed for GPS signal reception which exhibits 25 dB of gain and high immunity to detuning. The GPS configuration retention and a short time to first fix is possible due to a backup lithium battery. Two serial ports are dedicated by the microcontroller to communicate with GPS and AHRS using the RS232 communication protocol. A third serial port that converts TTL logic levels to RS232 standard levels is used for debugging purposes. It can be internally connected to the GPS or AHRS for debugging with their OEM software. A GFSK transceiver is employed to exchange information with the other devices such as the main capsule, base station and cutdowns. This communication

channel will be handled on the UHF ISM band thus, a monopole antenna was built and tunned to 869 MHz using a Vectorial Network Analyzer (VNA). Since the radiation pattern of a monopole has a null along its axis, it was placed in the opposite side relatively to the GPS antenna to avoid jamming caused by the GFSK transceiver harmonics. Microstrips of 50Ω are used as transmission lines between the antennas and the respective devices. For the 1.6mm thick glass fiber substrate (FR4) with an ε_r of 5.4, these lines are 2.61mm wide.

A micro SD card running a FAT system logs the relevant flight parameters. It shares the SPI bus with GFSK transceiver and apart from the flight information it saves, this memory will be also used in the future to store a low resolution landing spot grid for the case of communications failure. In this case, Drone figures out that it is unable to exchange information and it will enter in standalone mode. The recorded flight information is essential to improve the system model. A simple push-button stops the read and write access to the card, ensuring a secure ejection. Three sail winch servo motors coupled to the pulley shafts form the actuators. The microcontroller drives the three servos using pulse-width modulation (PWM). In order to prevent a mechanical jamming, it also limits the maximum travel available. Each servo provides a torque of 1.27 N/m which translates into 1.08 N using the 22 mm diameter pulleys. The ability to turn off the servos increases the battery life time which is useful for the climbing stage of the flight.

The airspeed information is essential when it equals the penetration speed of the wing. In this situation the GPS would show a stationary position making it almost impossible to figure out if the platform is still flying. The static pitot tube was built using differential and absolute pressure sensors. One rubber pipe facing the apparent wind serves as intake at the exterior of the Drone. The other tip of this pipe is then attached to port A of the differential pressure sensor whereas port B senses the static pressure. The differential pressure between port A and B represents the dynamic pressure that can be translated in airspeed if the air density is already known. The barometric (absolute) sensor is used to compute the needed air density and can also be an altitude indication backup in case of GPS failure. Both sensors are enclosed in the styrofoam apart from the other components to confine the low temperature to which they may be subjected. A pitot tube is preferred to an usual anemometer since it has no moving parts or a fragile shape which could become damaged during the landing. It is placed perpendicular to the mean air flow to reduce measurement errors **??** The measurements of pressure are possible through the I2C bus that also permits the communication with the temperature and power monitoring sensors in the PSU board. The latter ones are capable of voltage, current and power calculation using a sensing resistor. For debugging purposes, the CPU board is equipped with its own voltage regulator allowing a standalone operation from a common workbench power supply. Placing this regulator away from oscillator equipped devices ensures that the influence of PCB temperature changes are minimal. A bus carrying power, I2C protocol and the PWM signals connects the CPU and the PSU. Among the PSU connectors for servos, batteries and main bus, there is a connector for the general power switch which controls both battery systems.

The PCB's made in the context of this work started by being designed with the Multisim. This specialized software allows the user to build and simulate any generic electronic circuit. However,

Figure 3.6: Drone CPU

no simulation was made, since this software was only used for design purposes. The design process was always restrained to the components that could be obtained by a distributor such as Farnell or in rare exceptions from hobby orientated websites like Sparkfun. Surface mount design (SMD) components were used whenever possible to reduce the overall size and weight. After this process, a PCB layout was created using a printed circuit board layout and routing software called Ultiboard. This application uses the *n*etlist exported from Multisim and displays to the user the real connections that must be made between each component. Then, the routing process takes place by creating physical traces made of copper to interconnect the desired components. Whenever needed, the traces can switch from one layer to another using connection holes drilled in the subtract called vias. The choice of this two tools is related to the fact that they are in the leading edge of this kind of software, the availability at the faculty and the author's eight years of experience with it. Whenever was possible, the traces width were maintained no thinner than 0.3 mm. Traces that may handle higher currents were designed to be wider in order to maintain a low voltage drop when peak currents are required. Measures against RF disturbances were also taken such as short traces, ground planes in non-routed areas, low resistance ground paths and low internal resistance capacitors in key points.

The printed circuit boards for the Drone CPU and for the Modemrouter, which will be presented later, were produced personally by the author using the photographic method. The process begins by cutting the material to be used. It is made of a fiberglass subtract called FR4 covered by a thin sheet of copper on each side. These boards may already come with photosensitive varnish or it may be applied by the user using specific aerosol spray. A file containing only the drill locations

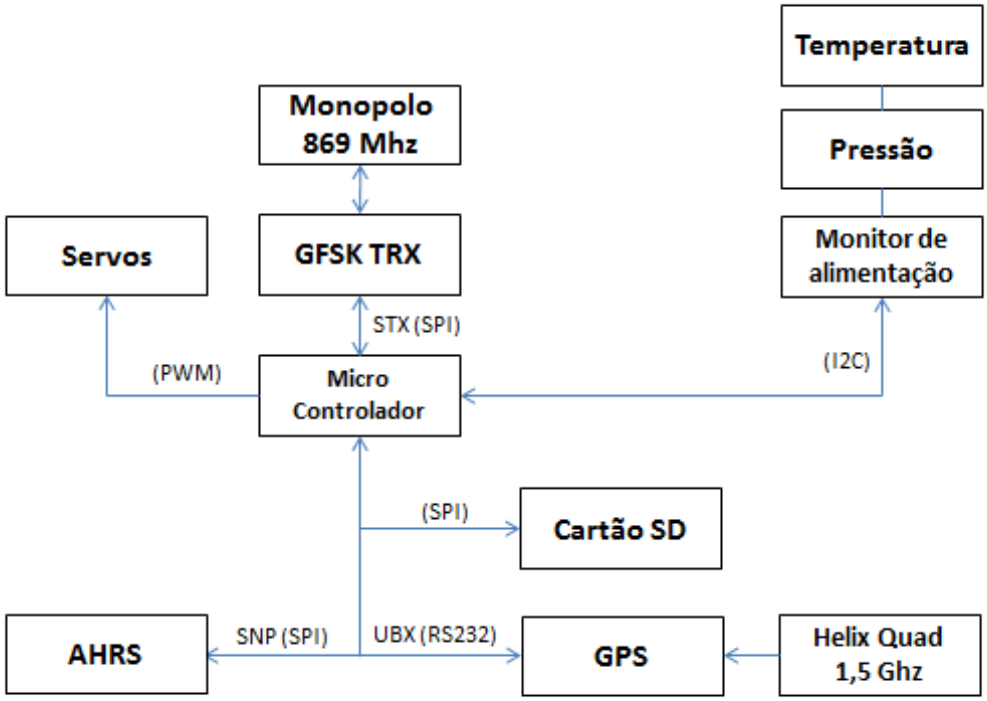

Figure 3.7: Drone System Breakdown

either for vias or for through hole technology (THT) components pads is exported from Ultiboard. This file is then transformed into G-code which is a standard numerical code that states the precise coordinates where the CNC machine should execute each drill. The prepared board is mounted in the CNC work table and a 0.3 mm drill bit executes the vias while a 0.85 mm drill bit executes the THT pads. Each layer of the designed layout is printed to a transparent or at least translucent media such as cellulose acetate or tracing paper. These prints are glued to the board in the corners and aligned using the drills as reference. This set is then exposed to ultra-violet radiation for about three minutes. During this time, the varnish areas not protected by the ink in the transparency will become sensitized. A sodium hydroxide solution removes the sensitized areas and maintains the desired traces. Finally, the copper in the non protected areas is corroded with ferric chloride. A transparent varnish is then applied to protect the copper from oxidation. After this the components are soldered by hand with a soldering station. The figure 3.6 shows the Drone CPU assembled.

3.2.3 Software

This section comprises the implementation of the algorithms running inside the CPU either to control the wing or communicate with the surrounding devices. Figure 3.7 describes the Drone system breakdown. At the startup a boot sequence configures the MSP430 peripherals such as

the clock system, UART's and timers as well as the GPS and SD card. To build an efficient code capable of run in the MSP430, all the routines are interrupt driven either by the reception of characters in the case of serial communications or by timers that periodically drive its execution. The GPS is configured to output the UBX proprietary format since NMEA protocol doesn't carry all the needed information. At a rate of four measurements per second, it transmits data such as actual position, velocity vector, time and quality of the estimates which are then used for the navigation loop. The coordinates are expressed in longitude, latitude and height whereas the velocity vector comes in north, east and down. In the other hand, the AHRS module makes available the roll, pitch and yaw angles at a rate of 20 Hz. The microcontroller receives and parses the relevant sections of each message. Gathered data and control variables are organized and stored in structures with the most recent information available. These structures can be uploaded and downloaded from Drone using a protocol specially developed for this application called STX. The most relevant structures are saved into the SD card each two seconds. It is implemented a FAT file system using a free generic library available on the web. This library works over low-level functions operating the SPI mode of the SD card. The information is stored as a comma separated values (CSV) format to an easy import process. Using the GPS data, the system estimates the flight phase. This parameter informs if the platform is on ground, climbing, flying with the round parachute or flying with paraglider. The position of the three servo-actuators is updated four times per second. This PWM signals are generated without CPU intervention. The MSP430 timers are able to control individual outputs and this can be used to produce the the PWM signals. The CPU interacts with the timer only if a new servo position is desired.

Also interrupt driven, the temperature, pressure and power monitoring sensors are read and the values are stored in the respective registers twice per second. The airspeed is then calculated using a pitot tube. This method of air speed measurement employs a differential and an absolute pressure sensors. It relies on the simplified Bernoulli's equation:

$$p_t = p_s + p_d$$

The static portion p_s represents the pressure of a stationary fluid. In this case, the fluid is the air inside the Drone which is sensed by the absolute sensor and by one of the ports present at the differential pressure sensor. The dynamic pressure p_d is the component added to the static pressure due to the movement of the fluid. The total pressure p_t is sensed by the remaining port of the differential sensor using a pipe connected to the exterior of the capsule. Thus, the differential pressure sensor outputs directly $p_t - p_s$. Given this, the airspeed can be calculated using:

$$v = \sqrt[2]{\frac{2(p_t - p_s)}{\rho}}$$

where

$$\rho = \frac{p}{R \cdot T}$$

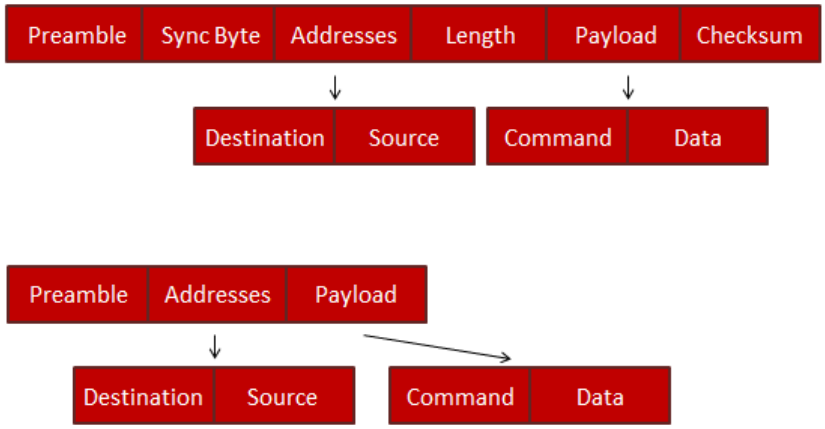

Figure 3.8: STX version 1 and 2

R is a fluid specific constant which in the case of the air is 287.058 $J/(kg \cdot K)$. Unlike the barometric sensor, the differential sensor is capable of returning calibrated measurements of pressure. Therefore, in the setup stage, the factory computed correction coefficients of the first sensor are loaded. Subsequently, at each absolute pressure reading, a corrected measurement is calculated using a second order polynomial that ensures a good accuracy over a wide range of pressure and temperature values.

In order to establish a small network to interconnect the system, a new communication protocol was developed. The STX protocol implements four types of packets and with a few exceptions, the packet type can always be "set", "get", "response" and "broadcast". A set packet writes data in the destination structure. A get command requests the remote structure to be reported to the source. The answer to that request is sent as a response packet. The broadcast type is a periodically sent packet without previous request. The available commands represent flow control messages, the transfer of complete structures and actions. The latter one refers to either an order such as "activate cutdown" or change a specific variable within a structure. The protocol consists on a generic preamble followed by an addresses byte, a command byte and an optional data payload section. The messages are addressed by reserving the most significant four bits for the destination address and the remaining four bits to the source address. Within the command byte the two most significant bits specify if it is a set, get, response or broadcast packet while the other six bits represent the command itself. The length of the data payload section depends on the type of packet and on the command. Flow control messages are always a set command without data payload and can be "acknowledge" or "not acknowledge". In spite of being recognized by the system, these messages are not currently used. This was kept for a future protocol upgrade where the reception of the packets may require confirmation. A structure packet type consists on the command byte that works as an identifier for the structure followed by the serialized structure itself. The data payload section is always empty in a get packet. Two versions of this protocol are available

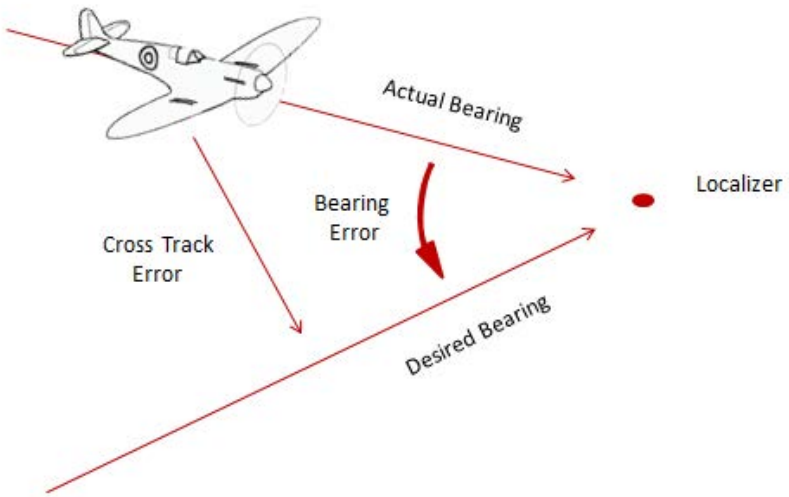

Figure 3.9: Localizer

(Figure 3.8). The first one is intended to be used with the GFSK transceiver, taking advantage from the encapsulating capabilities it offers. Version two is used in other communication mediums such as USB and SPI.

3.2.4 Operating modes

Three different operating modes are available in this system: Manual, Autopilot 1 and Autopilot 2. In the manual mode, as the name suggests, the paraglider is fully maneuvered by the user using a joystick. The ground station software interprets the joystick movements and sends that information to Drone where the servo-actuators are actuated accordingly. This can be done with the platform in sight or using either the ATV reception or a Google Earth interaction feature that will be explained later. The autonomous operation of Drone is instantiated two times leading to the autopilot 1 and autopilot 2. Since they are similar, the designation autopilot without the reference to the number will be used for explanation purposes. Although five autopilot types are planned, due to time restrictions only four were implemented. In the first type, the system follows an heading and a sink rate the user should provide. The second autopilot type is a variation of the first where heading is replaced by course. In aviation, one of the most used navigation methods uses a spacial point (localizer) and an angle of arrival (Figure 3.9). This defines the one point and bearing autopilot type (third method). In the last implemented type, the user specifies two points instead of one. In fact, in both types the user is providing an infinite line that crosses the localizer in a given direction. This is the desired path until the operating mode is changed. This can be done manually by the user or automatically accordingly to a set of three flags. In each autopilot, the flags "ready", "hold" and "recycle" may be set. Ready means the autopilot can be

promptly executed. When the platform crosses the last point of the localizer, which is also the first one in the case of one point and bearing localizer autopilot type, the system considers the current autopilot is concluded if the "hold" flag is not set. If that happens and the other autopilot instance is ready, the system switches the autopilot instance automatically. Unless the flag "recycle" is set, after the conclusion of an autopilot, the "ready" flag is cleared. In this case, the autopilot can not be used anymore without user intervention. The "recycle" option allows the user to insert a pair of localizers, whose lines are parallel but in opposite flight direction, leading the platform to a spiral motion. This scheme works well on a situation where the wind speed is less than the wing penetration speed. Otherwise, the platform is not able to reach to one of the localizers making the spiral movement impossible. The fifth type of autopilot called *S*piral would overcome this problem by inserting a drifting component coherent with the wind into the localizers.

3.2.5 Control algorithm

One of the most important functions is the autopilot. Its role is to manage the platform towards a target. Four different types of autonomous flight are possible: heading, course, one point localizer and course or two point localizers. First of all, the distinction between heading and course must be made. Heading refers to the direction that Drone's no se is pointing. Course is the direction of the path that the platform is describing. An heading or course oriented flight uses as reference a specified angle whilst uses as feedback the compass (yaw) or the GPS course respectively. Ideally, both are equal in a null wind condition. However, the presence of wind may induce a lateral slip. Activating one of these two autopilot makes the system take control of the servo-actuators. The angular velocity ω or, in other words, the control lines displacement come from the expression:

$$\omega = \frac{-HK_4 \cdot Hdg'_e - HK_2 \cdot Hdg_e}{HK_3}$$

HK_x denotes the coefficients empirically tuned which are stored in a structure and can be changed at any time to modify the control responsiveness. Heading error and heading error variation are represented by Hdg_e and Hdg'_e respectively. Although making the system sensitive to the error variation improving the reaction time, the derivative factor can cause instability if not correctly weighted. The control actions are computed four times per second providing smooth transitions. The expression above handles only the horizontal component of the autonomous flight. The vertical component b, which is common to all autopilot types, is given by:

$$b = \frac{-VK_0 \cdot SinkRate'_e - VK_1 \cdot SinkRate_e}{VK_2}$$

In the horizontal domain of a localizer autopilot type three different errors may be present: cross track error, heading error and bearing error. The cross track error (Xt_e) is the distance between the actual position and the projection of that position in the desired path. The difference

between the actual bearing and the desired one is called bearing error whereas the heading error takes into account the wind effect on Drone's attitude. A slightly different method can be used: a two points localizer. In this type of autopilot, the user may enter two spacial points and the software calculates the respective desired bearing. After that, it behaves as it was a one point and bearing operation.

$$\omega = \frac{-HK_4 \cdot Hdg'_e - HK_2 \cdot Hdge_e - HK_1 \cdot Xt_e - HK_0 \cdot \int Xt_e}{HK_3}$$

The expression above differs from heading and course following in what concerns to the cross track error. Otherwise, it wouldn't correct its path and would miss the localizer. The cross track error, distances to the points and the computation of the desired bearing in a two point localizer relies on an already developed routine by Prof. Sérgio Reis Cunha. These calculations are executed at a rate of 4 Hz. Due to the lack of sufficient flights, there isn't still enough data to model the system. This method works well but phenomena such as the pendulum effect and wing behavior with mass variations are not taken into account. The autopilot has two phases - approach and following. In the approach phase, the platform heads the ideal path at an angle α defined by

$$\alpha = arctan\left(\frac{min(Xt_e, Cd)}{Cd}\right) \qquad |Xt_e| \quad \in \quad \left]+\infty, \frac{Cd}{5}\right[$$

where Cd is the value of the Convergence Distance register. When the cross track error is under the threshold defined by $\frac{CD}{5}$, the phase switches to following mode. In the following mode the algorithm uses the ideal path direction as reference. This ensures that the platform takes a shorter route towards the target and a smooth transition between the two phases.

3.3 Main Capsule

The main goal of STRAPLEX project is to provide a platform to carry experiments to the stratosphere which will be recovered after landing. This capsule has an hexagonal shape with faces 308 mm long and 380 mm high. It is made of Styrofoam with a thickness of 30 mm which provides good thermal insulation and robustness against landing impacts. One of the faces has a window used for video capture from the interior which is relayed to the ground station using an ATV link. Inside the capsule, there are four separate layers stacked with different functions. From top to bottom, the first one houses a ground plane with the VHF, UHF and GPS antennas while the second layer is reserved for the experiments. The last two layers house the electronic equipment and the batteries respectively to maintain a low center of mass. The electronic equipment consists on amateur-radio transceivers, GPS receivers, modems, data acquisition module and a processing unit. The position of the platform is periodically reported to the base station by different means. The primary localization system sends position data through the UHF transceiver

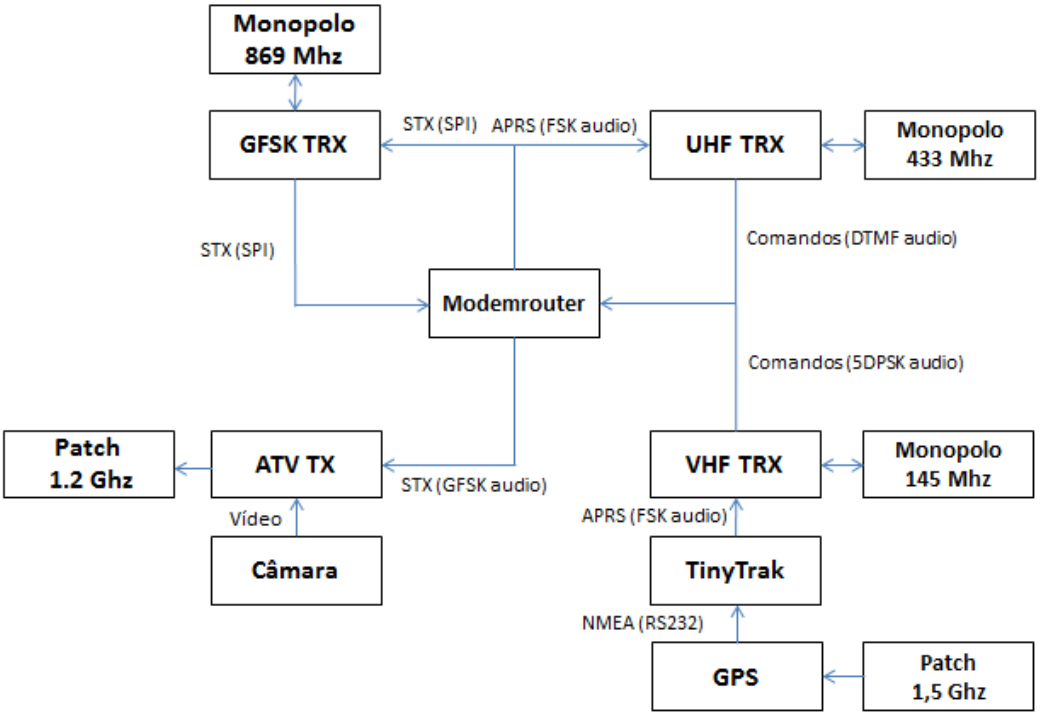

Figure 3.10: Main Capsule System Breakdown

over the automatic packet reporting system (APRS), which is an amateur radio-based network for information exchange of immediate value in the local area. In other words, this system allows to spread messages, alerts and bulletins over a network made of amateurs radio transceivers. Each packet irradiates from its source jumping from a node to another node until a maximum number of jumps is reached. In fact, some of these transceivers also relay the packets across the internet, making them available globally. The interesting feature which makes APRS useful to STRAPLEX is the possibility to add the station coordinates to the packets. These packets may contain on board data such as battery voltage or temperature. TinyTrak is a device that encodes the NMEA messages received from a standard GPS receiver into APRS packets ready to be sent. The redundant localization system consists in one of these devices connected to a dedicated GPS receiver and to the VHF transceiver. The power supply is also independent otherwise a short circuit in the main battery set would affect the redundancy of this localization system. The color camera injects PAL video signal into a 1.2 GHz modulator which is then followed by a 30 dbmW amplifier. The ground plane of the ATV antenna is located under the batteries with the monopole pointing down.

The Drone integration process into the platform required modifications on the main capsule. The need to create a channel to exchange data with the controller in addition to the existent ones yield to the design of a new module. Figure 3.10 shows the main capsule system breakdown being described. In order to allow a good processing capacity and a considerable amount of communi-

cation ports, the Modemrouter module is composed by three microcontrollers - a main one and two auxiliary. The auxiliary microcontroller 1 handles a DTMF decoder and a MFSK encoder that injects telemetry in the ATV audio channel. In the other hand, the microcontroller 2 decodes a 5DPSK modulation which will be received through the VHF transceiver. In the following sections these decoders and encoder will be explained. Each one of these two devices provide two RS232 serial ports, one port that can be configured in SPI or I2C mode and two GPIO which can be internally connected to an analogue to digital converter (ADC). One12 Bit digital to analogue converter (DAC) with parallel interface is also connected to each device. A fourth serial port is reserved for the system main bus which interconnects the three microcontrollers. The main microcontroller handles the routing functions of the packets coming and going to the other two devices and a GFSK transceiver. When a packet is decoded, an interrupt is sent to the main microcontroller. Then, through the system main bus in the case of the other two microcontrollers or by a dedicated SPI port in the case of the GFSK transceiver, the packet is exchanged. At the main microcontroller, accordingly to the destination address, the packet is forwarded to the correct device. This microcontroller also provides an USB port that can be used as routing path to a computer while the other four RS232 ports present on the Modemrouter may be used to connect GPS or TNCX modules.

3.3.1 Data uplink - 5DPSK

During a flight, several commands may be sent to the platform. Actions such as trigger the cutdown, select a landing spot or even control manually the paraglider may be taken. The GFSK transceiver operates at 19200 Kbps using a GFSK modulation and therefore, at greater distances, may be not possible to communicate with it. Since human voice doesn't include meaningful information at higher frequencies, the most common amateur radio transceivers use a very limited bandwidth in the order of 3 kHz. With this in mind, a FM UHF channel driven by a 5DPSK modulation scheme is employed to transmit basic data to the platform. This method allows the ground station to transmit basic control information taking advantage of high power amateur radio transceivers. Moreover, the differential operation decreases the computational complexity. This scheme employs five possible symbols evenly spaced in terms of phase. The first symbol (0^o) is used only for packet synchronization purposes while the remaining represent four combinations of two bits. Each packet is composed by 10 symbols starting with synchronization followed by six symbols of data and ending with three of checksum. The checksum segment carries the first six bits of data XOR-ed with the remaining six. Therefore, the twelve bits of data can assume 4096 possible words. These are divided in ranges to which a particular function is assigned. For example, the range from 0 to 63 indicates the main servo position whereas the range from 456 to 487 specifies the sink rate. Several words are reserved to execute actions such the engagement of the autopilot 1. Running on a base station computer, a Simulink model implements the 5DPSK modulator using the sound card. The sound card output is then connected to the radio enabling the transmission of the packets. A joystick connected to the same machine enables the manual control

of the Drone effectively bypassing the autopilot. Sink rate and heading or course can be entered using the hat switch while other functions are available using buttons on the joystick controller.

From the demodulation point of view, the auxiliary microcontroller 2 is responsible for demodulate, decode and send the data to the main microcontroller. The signal received from the radio is initially sampled at 2 kHz with a resolution of 12 bits. The samples are stored in a circular buffer and retrieved to filtering and decimation every time the buffer reaches or exceeds the number of elements needed to compute a filtered sample. Since the unfiltered samples are used alternately to multiply by the real and imaginary components of the filter, the sampling frequency decreases to 1 kHz. Thus, after the decimation, the signal is divided in real and imaginary parts. Then, the synchronization mechanism finds the optimum timing to recover the symbol by searching phase transitions. After centering the window on the transition, the accumulated values for the imaginary and real parts are compared to a look up table that contains the expected real and imaginary parts of each symbol. The two bits that the decoded symbol represents are concatenated to the previous ones already decoded except in the synchronization symbol case. This process is repeated ten times to recover the whole packet. The decoded data is validated by comparing the first two groups of 6 bits after the synchronization with the checksum. The received command is then translated into an STX packet which is then transferred to the main microcontroller in order to forward it to the correct destination.

3.3.2 Data uplink - DTMF

DTMF stands for Dual Tone Multiple Frequency and specifies a standard signaling system to transmit up to 16 distinct digits over a given channel. This system is widely used in the common telephone service (also called POTS) and as activation tone in the amateur radio repeaters. Thus, many amateur radio transceivers are able to modulate any desired tone which may be useful for sending basic commands if the other available communication systems fail. It consists of two different frequencies (tones) from two sets of four whose combination results in sixteen possible digits. Since this is a reserve system, the commands available are very basic and don't need to be quickly transmitted. In fact, the operator may hold down the button of the desired tone for several seconds to make sure the command is received.

This decoder starts with an ADC sampling, converting the received audio signal at 6 kHz on the auxiliary microcontroller 1. Then, a real discrete fourier transform is ran at each set of 512 samples converting the signal to the frequency domain. If this signal at any point reaches a given threshold, it is calculated the nearest valid DTMF tone. Since the frequency domain signal is divided in 512 bins, the minimum separation between tones, which occurs with the 697 Hz and 770 Hz frequencies, is five bins. This ensures reliability against frequency shifts which otherwise could cause a tone to be confused with another one. To prevent transient signals from activating a given digit, the same digit must be decoded ten times in a row which corresponds to a signal presence of about one second.

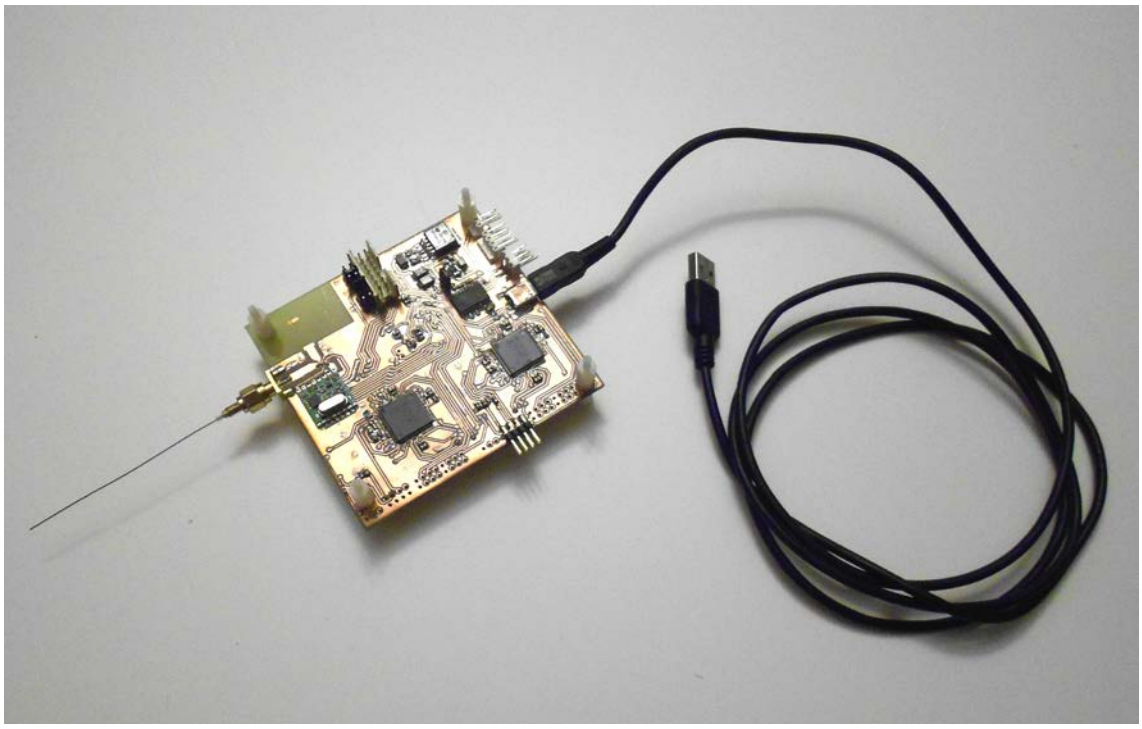

Figure 3.11: Modem Router

3.3.3 Data downlink - GFSK

Taking advantage of the unused audio channel of the ATV transmitter, the auxiliary microncontroller 1 injects telemetry data on it using gaussian frequency shift keying (GFSK) modulation. This telemetry channel allows a comparatively high baud rate providing the option of closing the control loop at ground station level, which will be important during the modeling stage.

The telemetry data is routed to the auxiliary microcontroller 1 using the main bus. After being parsed, the useful information is extracted from the packets and sent over GFSK. This routine converts each bit of the data payload in a tone. A 12 kHz tone means a logical "1" while a 6 kHz tone means a logical "0". This encoder uses a sampling frequency of 96 kHz which results in a bit rate of 6000 baud assuming that at each symbol there is, at least, one complete cycle. For a low computational cost, the tones with the gaussian filter already applied are stored in eight look-up tables that contain all possible transitions between three consecutive bits. A digital to analog (DAC) converter outputs the audio signal with a peak-to-peak voltage of 1 V. This signal is then injected into the ATV audio channel.

In the future, this may be replaced by other modulation schemes with higher baud rate. Multi frequency shift keying (MFSK) or several quadrature phase shift keying (QPSK) channels are proposals still in discussion. Since this signal is modulated over a FM channel, the modulation robustness is not so relevant. The predominant factor in the ability to decode the packets will be the initial FM demodulation.

3.3.4 Cutdown

The platform often flies to Spain air space where is no longer of the responsibility of the Portuguese authorities. If this is the case, a previous international authorization is needed. In the uncommon circumstances (but possible) of a rejected authorization, the STRAPLEX ground control must to be able to abort the flight. This is also true if the platform is heading to land on an unrecoverable region such as the sea. The cutdown device has the function of separate the capsules from the balloon which provides lift. In the earlier versions of this project, a pyrotechnic device was coupled to the line that is attached to the balloon. It consisted of a low value resistor to act as electric match that is embedded in the composite of phosphor. When applied enough power for a given time, the resistor rises its temperature up to the ignition temperature of the composite. After ignition, the line burns locally separating the two parts of the platform. However, the low effectiveness of this system led to several separation failures with the balloon landing attached to the platform. One of the problems detected was the inconsistency of the burning mechanism which sometimes was not hot enough to cut the line. On the other hand, the physical electric connection between the cutdown device and the main capsule is prone to be damaged due to the parachute agitation on the first minutes of the descent.

Adding a parafoil increases even more the relevance of a reliable cutdown device. In the case of failure, the canopy may take an asymmetric shape or have its control lines jammed due to the balloon remains. For these reasons, a modification of this device was carried out. The pyrotechnic method besides being unreliable, is also dangerous if the device is accidentally activated while it is being manipulated. Thus, a mechanical approach was preferred. The new cutdown can be split in two subsystems: a generic trigger system connected to an application specific release system. The trigger system is composed from a GFSK transceiver, a microcontroller and a servo. The GFSK transceiver makes it possible to access the STX network and receive the cutdown command. The microcontroller interprets the packets and acts accordingly. If a cutdown command is received, the microcontroller induces rotation in the servo mechanism. The releasing system depends on the application. The first cutdown system, which separates the balloon from the platform, consists on a lever mechanism that without trigger system intervention remains holding the line. The servo-motor, which is attached to a sheet of soft acrylic , has a 15 mm long arm with five fixing holes. One tip of a line is tied to the middle hole while the other is attached to a lever made of the same material. Due to the location of the lever pivot, the mechanical advantage is about eight times. Touching the smaller segment of the lever there is a latch that holds the hang line into position. When the microcontroller receives the cut order, it changes the PWM of the drive signal leading to a 180^{o} rotation of the arm. This rotation pulls the line and therefore the lever about 2 cm. In this position, the latch is disengaged and the hang line separated. On the other hand, the second cutdown deploys the wing that is trapped inside a bag. This bag has a rectangular shape with rounded upper corners. The center is reinforced with nylon straps that hold the tractive force before the wing deployment. This bag is kept closed with a pin that holds a strangulation line that cross a set of eyelets around the opening. If the trigger system is enabled, the pin is pulled off and

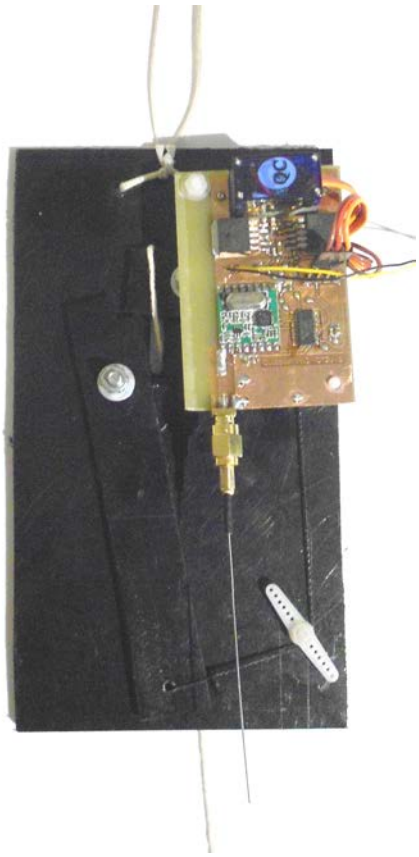

Figure 3.12: Cutdown with lever mechanism

the canopy deployed. This allows to have a cutdown system highly versatile that can be used in the future to other purposes.

Chapter 4

Ground station

The STRAPLEX platform requires to be closely monitored during the flights. A fixed station is configured, usually, at the launch location (Figure 4.1). It is composed by a computer that gathers information about the platform position and status. It uses amateur-radio transceivers to receive the APRS packets on the VHF and UHF bands. They use monopole antennas tuned to each band mounted in the top of a mast four meters above the ground. It is also possible to use this transceivers to send DTMF tones or the 5DPSK modulation over their audio. A GFSK transceiver, similar to the ones that can be found in the several modules of the platform, has its output amplified to 33 dBmW. An yagi antenna mounted on a rotor is used both to transmit and receive the STX packets. Along with the yagi antenna there is a 1.2 GHz antenna to receive the ATV broadcast. The signal is amplified and delivered to a suitable analog satellite receiver which displays the image in a screen. The position of the rotor is controlled by the computer which uses the received telemetry to point the antennas in the best direction. A simplified system that includes only APRS decoding capable transceivers is also mounted in a vehicle to help in the rescue process.

4.1 Base station GFSK transceiver

Due to the reduced distances, the STX network nodes communication on board of the platform is not a problem. In the worst case, the maximum distance between two transceivers on the platform is about 10 meters (from the main capsule to the first cutdown). The same does not happens with the base station transceiver which can be more than 100 km away. A high baud rate communication link between the ground station and the platform is always useful. It can be used to upload and download data more easily and often. Taking 150 km as the maximum distance from the base station to the platform, the 20 dBmW of output power on a monopole antenna makes it impossible to establish a link. The solution was to increase the output power at the base station by adding a power amplifier to the base station transceiver. This is not applicable to the on board transceivers due to power restrictions.

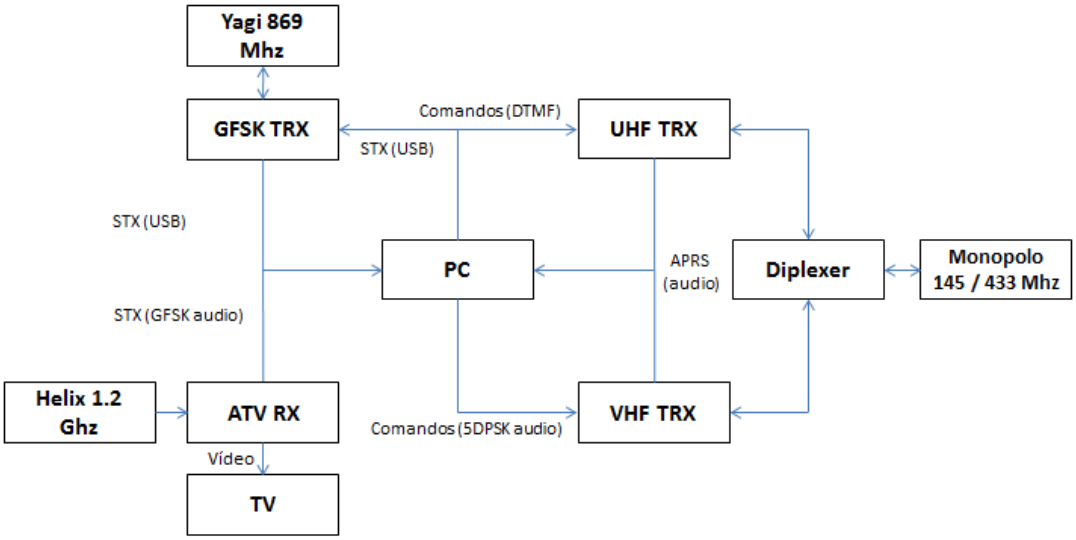

Figure 4.1: Ground Station System Breakdown

Thus, a new PCB was made to house the components of the base station transceiver. A microcontroller manages all the operations with the GFSK transceiver and provides an USB support to connect to STX center, a software that will be explained later. The microcontroller USB module implements a communications device class (CDC) which emulates a RS232 serial controller after correct driver be installed. In fact, the base station transceiver only routes the packets from and to the STX center making the conversion between the two versions of the STX protocol. In the host computer, the interface software is similar to serial port programming. The receive and transmit operations share the same antenna. The transmission line between the antenna and the transceiver is swept employing a pair of RF switches. In the receiving path, a low noise amplifier provides the gain to compensate RF switches losses. While transmitting, the transceiver feeds an amplifier capable of delivering 33 dBmW to the antenna. The RF switches are digitally controlled by the transceiver. The USB port powers all the devices except the output amplifier which is externally powered. Due to the considerable high power requirements of the referred amplifier, a switched-mode power supply is employed to ensure an efficient and easy use of this device with a common workbench power supply or lead acid batteries.

For a 150 Km uplink at 869 MHz, the free space loss is given by:

$$L_{FS} = 20 \cdot log(\tfrac{4 \cdot \pi \cdot d}{\lambda})$$

$$L_{FS} = 20 \cdot log(\tfrac{4 \cdot \pi \cdot 15 \cdot 10^4}{0.3452}) = 134.7dB$$

Estimating a cable loss L_{Tx} of 1 dB and a antenna gain G_{Tx},G_{Rx} of 2 dB, the uplink budget P_{Rx} can be calculated as follows:

Element	Length (mm)	Position (mm)
Reflector	174.6	30
Radiator	162.1	99
Director 1	156.9	124.9
Director 2	155.3	187
Director 3	153.7	261.1
Director 4	152.3	347.4
Director 5	151	444
Director 6	149.7	547.5
Director 7	148.6	656.1
Director 8	147.5	770

Table 4.1: Yagi elements length and position

$$P_{Rx} = P_{Tx} + G_{Tx} - L_{Tx} - L_{FS} + G_{Rx} - L_{Rx} =$$

$$= 33dBmW + 2dB - 1dB + 2dB - 134.7dB = -98.7dBmW$$

Since the receiver sensitivity with this configuration is - 109 dBm for a bit error rate of 10^{-3}, the uplink margin is only 10.3 dB. For the complementary downlink, the received power is 13 dB lower which results in a negative link margin of 2.7 dB. These link margins still don't provide the reliability expected. Therefore, a directional antenna was implemented to enhance the link margins and it will be explained in the following section.

4.2 Yagi antenna

Several possibilities for a directional antenna were considered. However, the simplicity and gain at the frequency of interest led to the choice of a Yagi antenna. Using an available software called *Y*agi *C*alculator, the dimensions of the elements were calculated (Table 4.1). The antenna consists of an aluminium boom with brass elements across it at specific locations. The aluminium boom is drilled to accommodate the elements which are then held in place using screws. As the antenna is a balanced system, a balun is used to unbalance it. The balun is built from a single toroid winded with copper wire which is inside a box and fixed near the radiator. The elements were carefully cut and tuned with the help of a VNA properly calibrated. This antenna shows a theoretic gain of 13 dB. However, due to time limitations, the radiation pattern was not measured.

The GFSK transceivers on board of the platform are able to output a maximum of 20 dBmW which is 13 dB less than the base station GFSK transceiver. Thus, the link margin for the downlink is only 9 dB. In reality, this is not a big concern since the relevant data is relayed in the ATV audio channel downlink. Although the base station GFSK transceiver is able to output a maximum power of 33 dBmW, the GFSK transceivers on the platform have an output power of 20 dBmW, which is insufficient for a reliable bidirectional channel at great distances.

4.3 STX center

The requirements for having a fairly complex system easily operable led to the build of graphic user interface (GUI) to control the platform. This was done making use of Matlab capabilities to program GUI's. This software uses the STX protocol version 2 and accesses the base station transceiver through the virtual serial port created by the USB driver. Each time a packet is received and decoded, the respective register and display are updated. Figure 4.2 shows the typical appearance of this software. The window is organized in several sections, each one representing a different data structure. On the upper left corner, one of the most important informations can be seen: the navigation data. In this area is displayed the current Drone's position, attitude, speed and time. The coordinates are in the form of longitude, latitude, height and altitude, while the velocity vector is represented as north, east and down. Attitude data is shown as pitch, roll and yaw. Immediately below, GPS measurements quality informs the user if the navigation data is reliable. A large value in horizontal, vertical or speed accuracy means that the GPS has been turned on recently or has an obstructed view of the sky. The tracking status may be confirmed watching the Fix and Fix Flags parameters. A 3D fix and All Valid keywords in each register respectively, indicates valid coordinates.

On the lower right corner the operation status shows the current control mode, the modules that are working properly, the estimated received power, among other information. On the right, three different monitors report power status, temperature and pressure. They are further divided in a few instances for different sensors. On the center of the screen, wind forecast at different flight levels can be uploaded to Drone. This information will be used in the future to compute approach strategies that take advantage of different wind directions and intensities. The forecast section estimates the landing area for the case of cutdown triggered immediately and for a full flight. Below, in the Options box, the operator can activate or deactivate some Drone features. For example, Servos Lock disables the servo-motors whenever the Flight Phase is different from Down Paraglider. This allows energy saving since the servos are used in only half of the flight. The servos position and offset is displayed in the Servos area. In this section is also possible to adjust the servo-actuators offset to correct mechanical misalignments. Autopilot boxes are divided into Download and Upload. The Download box refers to the data currently loaded in the Drone registers. The new parameters that the user may want to update are entered in the Upload box. These parameters include point coordinates, sink rate and course. Since entering the coordinates is time consuming and prone to mistakes, there is the option of load Google Earth placemarks. Thus, the user can pinpoint several key locations in google earth creating a database of placemarks. Then it is possible to import the desired placemark into the STX center with no need of typing. Colors are sometimes used to make sure the user is aware of important aspects. For example, an autopilot in a green background means that is active whereas a check box in a red background indicates a warning. The Posture section displays path error estimates, time to end and other relevant information used in the guidance system. Control parameters can be changed in the tuning area. This section contains the control algorithm coefficients and some variables used

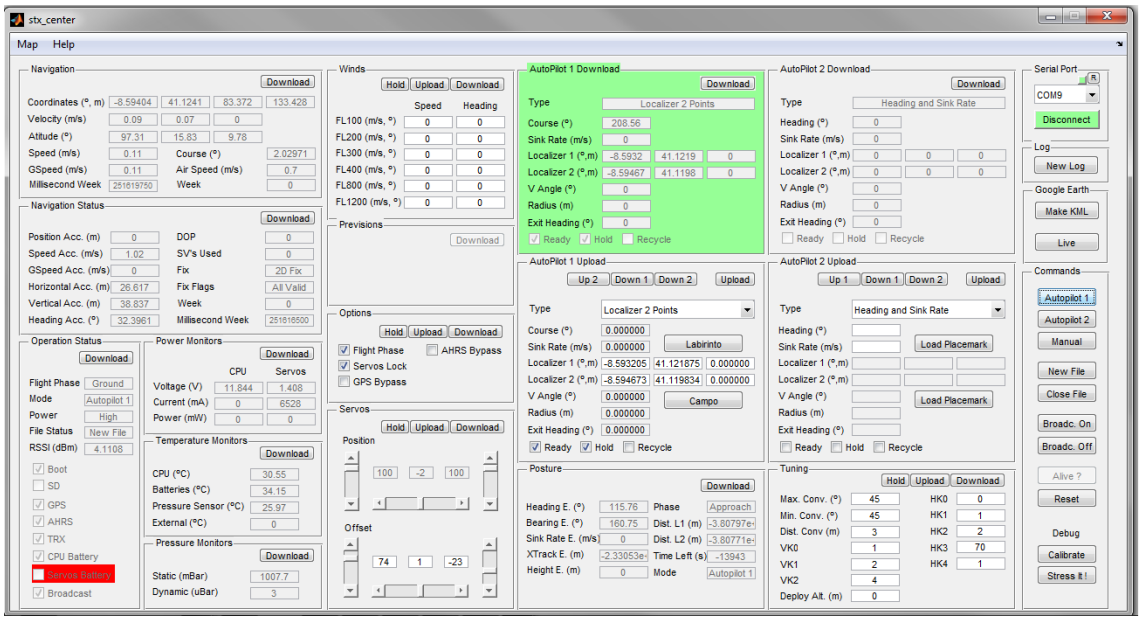

Figure 4.2: Graphic User Interface

as restrictions.

On the right upper side is possible to choose the virtual serial port to connect to the transceiver. The Connect button opens the chosen COM port. A log button allows create a file where all the received information is saved in CSV format. From a log file, the software is capable of building a three-dimensional path in Google Earth with periodic placemarks containing information such as time, speed and servo-motors positions. Another useful feature consists in using the location and attitude data to induce google earth to display what Drone is seeing. This enables the manual control of the platform without visual contact or even ATV reception. Taking into account that a high speed internet connection may be not available at the base station, it is possible to use google maps to track down the platform using the Map button in the tool bar. This map is updated every minute and the user may chose different zoom levels. A help section provides the user several notes about using the software. In the Command box the user may choose, for example, the operating mode. In manual mode, the software is able to interact with a joystick in order to control the Drone. At any time the user can upload or download the structures using the respective buttons with the same name. The structures may be automatically downloaded turning on the broadcast. Accordingly to their relevancy, in broadcast mode, the structures are periodically sent to the base station.

Chapter 5

Tests

This chapter comprises several tests performed to validate some subsystems. It starts with the study of the STX link under simulated circumstances and continues with the cutdown loading test. The last three sections describe detailedly the ground and flight tests executed to develop and evaluate the control system performance.

5.1 STX link

The STX communication channel is the primary system for exchanging information among the STRAPLEX platform system. On the other hand, a communication channel with the main station it is not essential but it is important. Therefore, a preliminary qualitative test was conducted to evaluate the maximum communication distance between two GFSK transceivers. The Modem-router was placed in Monte da Virgem which is a mount near the center of the Vila Nova de Gaia. Located at 230 m in altitude it is place of an astronomical observatory and several television and radio transmitters. Since the base station transceiver was not concluded at the time of this test, Modemrouter was used instead and the monopole antenna was alternately replaced by the yagi antenna to evaluate the performance of the system with each one. Mounted on a tripod, the yagi antenna in vertical polarization was pointed visually to the location of the other transceiver and confirmed using a compass. Drone, with its own monopole antenna, was used as the second transceiver and it was placed on the top of the Santa Justa mount at 320 m in altitude in Valongo, Porto. The distance between the two points is about 10.7 km in line of sight with no obstruction. Both transceivers were transmitting 20 dBmW at a frequency of 869 Mhz. The test consisted in updating structures and activating certain commands such as "broadcast on" and "broadcast off" to ensure that a communication was possible. Although the system performed well with both antennas, when using the yagi antenna the communication was a little bit more stable. After this, the distance was increased moving the Drone further to the mount of Santa Eufémia in Vila do Conde at a distance of 22.6 km from Monte da Virgem. With this configuration, a weak communication was only possible with the yagi antenna carefully aligned. However, this second site was only marginally above the horizon due to near elevations and tall buildings in the city of Porto. Another

Figure 5.1: First test from the first set visualized in Google Earth

issue relates to the fact that this highly urbanized area is in the same direction of Santa Eufémia could be a possible source of interferences.

5.2 Cutdown

The first cutdown system, which is composed by a trigger and a lever cutter, is intended to break the link between the round parachute and the balloon. When the cutdown command is executed, the servo-motor pulls a lever that releases a latch which is holding the line. It is supposed to tolerate, at least, the tractive force caused by the mass of the platform. The validation test for this device consisted on holding 100 N for 8 hours with a consecutive successful cut. This was achieved by hanging two 5 liter bottles. After the desired 8 hours, the cutdown was activated and the separation occurred without trouble. After the test, the reset command was issued with the mechanism returning to its holding position. The footage of this test is available in the website made within the scope of this work.

5.3 Ground tests

In order to validate the navigation, guidance and airspeed estimation systems, three sets of ground tests were conducted. For the first two sets of tests, the Drone without the canopy was mounted on the top of a car which was driven in certain areas. The areas were chosen accordingly to the requirements of each test and road safety concerns leaded to the execution of this tests during the night.

The first set of tests occurred in a residential area where the roads are aligned in a matrix style. This allows to perform several different paths with reasonable distances. The main goal was to validate the precision of cross track error and course error estimations and consequent control actions. In the first test, Drone was programed for course and sink rate autopilot type. The sink rate control is not evaluated in ground tests for obvious reasons and is always set to 0 m/s. At the starting point marked with A in figure 5.1, the course was set to 140º. Immediately after the simulated launch, the course error was estimated in -149º leading to 70% of travel to the right side. Thus, in the next intersection, the driver turned right and the error decreased to about -60º and 27% of travel. Since this particular street describes a soft curve to the right, the error continued to decrease to 0º. After that point moderate turns to the right and to the left induced small compensation actions as expected.

For the second test, both autopilots were used. Autopilot 1 was configured as a one point and course localizer with the coordinates of point B and a course of 80º. On the other hand, autopilot 2 was uploaded as a two point localizer from C to A. The car started from point A with the same direction as in the previous test. After the first right turn, the cross track estimate was -151 m and the control algorithm indicated a right action in order to intersect the localizer at 45º. During the approach phase, the car was steered accordingly with the control corrections and the cross track error decreased progressively. Three meters before null cross track error, the algorithm started to align with the first localizer making a moderate left turn and changing to the following phase. About 60 meter later, the desired point is achieved and the control changes automatically to autopilot 2. A cross track of -70 m and a course error of 180º induced 65% of travel to the left towards the localizer defined by the points C and A. After entering the following phase, the control algorithm maintained a straight line to the last point.

The purpose of the third test was to validate the autopilot recycle feature. Thus, the points F and B were defined on the autopilot 1 while autopilot 2 was loaded with points D and E. This test showed a consistent behavior with the previous one except when the point E was reached. When this happened, the control changed again to the autopilot 1 closing and repeating the circle.

This set of tests demonstrated a solid control algorithm in the horizontal plane. However, the canopy dynamics which may cause instability cannot be assessed with this method. This will be addressed in the low flight tests. After the analysis of the logs, it was detected that sporadic wrong coordinates were received from the GPS receiver. Measures against this momentary problems were taken. A position validation routine ensures that coordinates above or under certain altitudes or those that differ from the previous ones by a given value are considered invalid.

The second set of tests were intended to calibrate the pitot tube assuming a null wind condition. In this situation, the airspeed measured by the device will be the apparent wind caused by the motion. The sensor is placed on the top of the capsule centered with it. An advanced position relatively to the front of the capsule exposes the sensor to the landing impacts. However, a retreated position can lead to noisy readings due to air turbulence. With this in mind, four tests were performed to evaluate the measurements at two different speeds and distances between the tip of the pitot tube and the cutting edge of the Drone. The tests were conducted in a 200m straight road

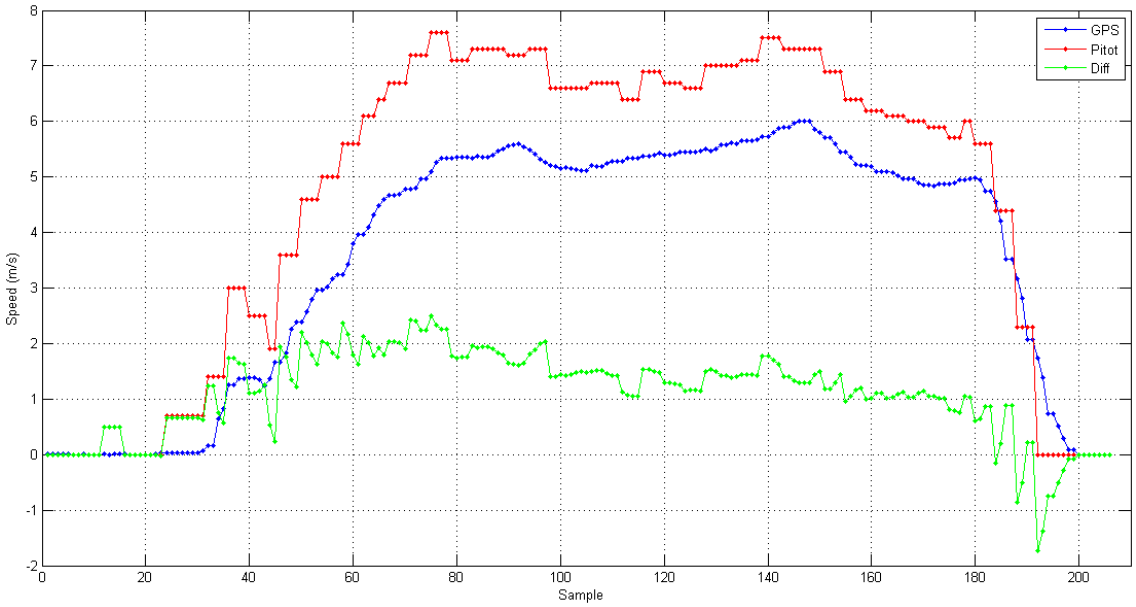

Figure 5.2: Measured Airspeed versus GPS Ground Speed

at 20 km/h and 40 km/h. Figure 5.2 represents the measured airspeed and GPS ground speed at 20 km/h with the sensor 50 mm ahead the Drone cutting edge.

In this figure, it is observed that the measured airspeed is proportional to the ground speed but not equal. This data was later used to correct the airspeed readings. Comparing the two locations of the pitot tube at both speeds, the retreated position demonstrated to be indeed more prone to turbulence and consequent noisy measurements. The absolute pressure sensor showed a good performance with a difference of less than 1 mBar relatively to the expected value.

The last ground tests set was executed on foot in the square in front of the faculty library. The aim of these experiments was to tune the control constants to achieve a good responsiveness and avoid oscillations caused by the pendulum effect. To do this, the autopilot 1 was configured for a 2 point localizer. The first point coincides with center of the department of mechanics building whereas the second point is centered with the stairs that give access to the B building. Then, a person holding the Drone in the hand serpentined along the line between the two points simulating the horizontal component of a lateral pendulum effect. Analyzing the control actions while doing such movements, the control coefficients were adjusted in order to avoid over reactions but without losing responsiveness. The coefficients empirically determined here were the base for further tuning in the flight tests.

5.4 Low altitude flights

Low altitude flights were made at the faculty to validate the controllability of the paraglider. Drone and the respective canopy were launched from the roof of the department of mechanics building several times to test each component of the control system. This kind launch consists on a person

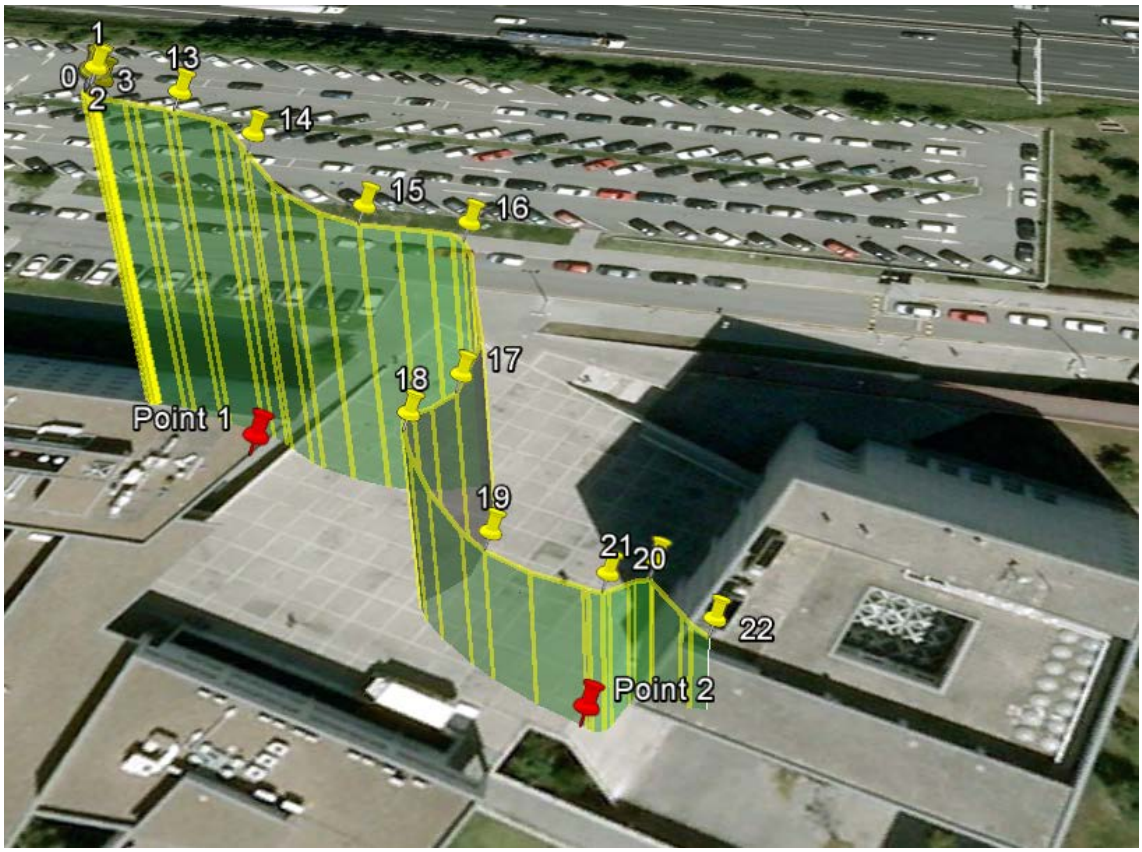

Figure 5.3: Longer Low Altitude Flight

holding the Drone with the wing open lying on the floor. After a short run, the wing rises and the Drone is dropped after the protective wall. First flights were made in manual mode to adjust the length of the four lines and to make sure that there was enough actuation capability to steer Drone in the desired direction. The system landed successfully in the square ahead and the wing proved to be fairly controllable and stable in a null wind condition. The launch procedure on the roof was found to be very critical in windy days. Head winds cause the wing to be dragged backwards not allowing a safe deployment of the Drone. On the other hand, tail winds require a higher launch speed to gain enough lift. This is difficult to achieve by a person running and holding the Drone. Cross winds can twist the lines and collapse the wing. Another issue is related to the pendulum effect triggered at the moment of the launch. Every time the capsule bounces forward, the angle of attack of the wing increases which results in a momentary increase of drag and decrease in horizontal speed followed by a sudden loss of altitude. The correct procedure is to wait for the wing to be right above the capsule to deploy it. However, even in a perfect launch, the height of the building is insufficient to make more than three 90 degrees fast turns. This fact restricts heavily the type, quality and duration of the flight tests. After mastering the launch technique, a set of flights in autonomous mode took place. The autopilot 1 was loaded with a two point localizer that connects the center of the department of mechanics building and the stairs that give access

Figure 5.4: Drone before landing

to the B building. Autopilot 2 was configured as a one point and course localizer centered in the same stairs pointing to 200 degrees. In this set, only the horizontal component of the autopilot was used. Drone was launched 9 times, with 4 successful flights, 4 flights with momentary wing collapses and an unexpected wing behavior which led to a 180^{o} turn. All wing collapses recovered naturally but the altitude loss made it impossible to correct the trajectory before landing. In some tests, it was found that tight turns also induce the pendulum effect. Besides the already explained decreased performance, the Drone movement in a direction different from the one it is progressing changes the course reported from the GPS receiver, causing erratic control actions.

The longer flight of this set is presented in the figure 5.3. The localizer points are marked red and the actual trajectory in yellow. All flights are recorded by a camera mounted on a tripod. In this particular flight, just after launch, it is possible to notice in the recordings that the wing was dragged east by a gentle breeze. The control executed a turn to the right to compensate and intersect the desired path. Five seconds after the right turn, the cross track error is canceled and a gentle left turn is executed heading directly to point 2. Drone landed after the stairs already in autopilot 2 mode. Figure 5.4 shows the typical appearance of Drone flying. In this picture is also

possible to see the protective cover that was employed to minimize the capsule damages during the tests.

5.5 Medium altitude flight

The flying time with the launches from the department of mechanics is plainly insufficient to test more complex trajectories. Finding a good location to conduct the experiments is not a trivial task. The launch site must be at a high spot with calm wind while the expected landing area must be clear of trees, buildings and watercourses. These conditions are not satisfied, for example, in Valongo or other nearby mountains. Serra da Freita in Arouca was the chosen place to conduct the medium altitude flights. The high terrain slope in several directions along with two kilometers long valleys make this mountain appropriate for this tests.

In the first expedition, three hours were spent finding the best place to launch the Drone. Power lines, unfavorable wind or lack of accessibility for Drone recovering were the main issues that made some launch sites unsuitable. A good area to perform the desired tests was found in the valley that ends in the village of Drave. Surrounded by higher mounts, this place is sheltered from the stronger winds and the vegetation is low enough to walk through it. The base station was installed in the south slope in order to have a better visibility of the area. Equipment such as a windsock and a camera were used to collect visual data of the flights. The first launches took place in the east side of the valley. However, the frontal winds that were felt in the afternoon made the launch attempts unsuccessful. In every launch, the paraglider, after progressing about three meters, was blown by the wind towards the launch site. This wind flows along the valley heading southeast. Another strategy was attempted in the west side of the valley which has a greater slope. Taking advantage from the wind direction and speed, the launch was performed parallel to the valley. After take off, the wind took the paraglider towards the center of the valley, as expected. Due to time restrictions, only two launches were possible in this configuration. In the first attempt, the system tried to compensate the direction but, in the meantime, it got stuck in one of the few trees of the area. After a successful retrieval, the second launch took Drone further but the impossibility of flying into the wind led to the progressive decrease in altitude without gain a height towards the center of the valley. It landed almost vertically at a distance of 50 m from the slope where it had been launched.

In the second expedition to Serra da Freita, other launch site was analyzed. Although the good slope in three different directions, Pena Amarela proved to have a denser vegetation than Drave and a more difficult equipment setup. Back to the place chosen in the first expedition, the launches were made from the west hill, where the best results were obtained in the last time. The slower wind increased the expectations of a longer flight. Figure 5.5 offers the perspective of the first flight from the base station. The autopilot 2 was loaded as a course and one point localizer that goes from the launch site to the center of the valley (red markers 1 and 2). There, it intersects the autopilot 1 which follows the valley to Drave (red markers 2 and 3). For the first 40 m, Drone flew in manual mode to create some clearance from the launch site. During this time, it moved

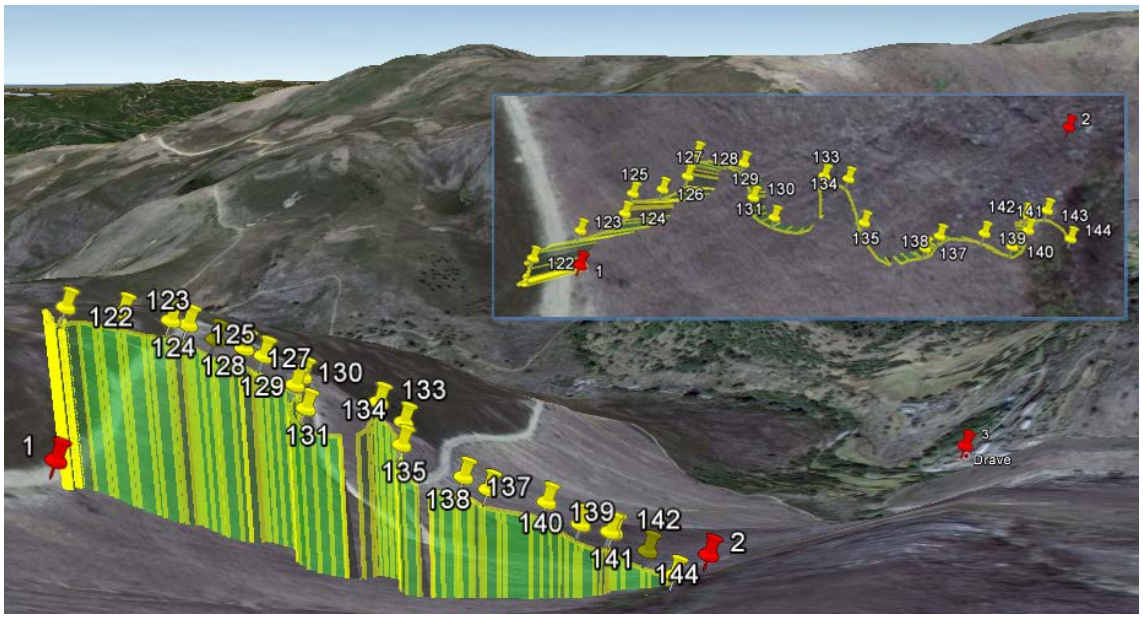

Figure 5.5: Medium Altitude Flight

perpendicularly to the valley facing the wind. At about ten seconds into the flight and 40 m of distance traveled, the autopilot 2 was engaged. The system tried to follow the localizer but the faster air masses diverted it to south, landing 160 m away from the launch site and 9 m from the intersection point. Indeed, the wind was strong enough to make Drone climb between the markers 133 and 134 in figure 5.5. From the collected data it is possible to realize that Drone tried to correct its trajectory but the impossibility of penetrate into the wind resulted only in oscillations along the path. The average speed was 18 km/h with a maximum of 35 km/h during a momentary wing collapse. The average glide ratio for this flight is 2.8:1 with a mean vertical speed of 1.8 m/s. A second flight in manual mode was performed in the same conditions. The pilot tried to progress in direction of Drave but Drone landed 45 m away from the first attempt.

In order to attempt a better flight, the launching location was moved for a slope at south from Drave. Thus, it was expected that the moderate wind coming from north would take Drone towards the destination. However, it was found that the wind was weaker in the new launching site. After two unsuccessful launches, the GPS antenna broke. With the navigation system inoperative, no further launches were executed.

The footages made from the base station (500 m away) of first and second flights can be seen in the website under the name of "Drave 1" and "Drave 2" respectively.

Chapter 6

Final remarks

6.1 Difficulties encountered

The extensive work required within the scope of this dissertation forced to begin the work in mid-October. This work extended by the nine following months. Many setbacks occurred during the development, with emphasis for two particular situations. The delivery of a group of aluminium parts that were ordered to the department's workshop in December, had been pending till April due to a maintenance operation in one of the machines. Since that at this time, only one piece was concluded and with no perspectives of concluding the remaining in a near future, the rest of the work was canceled. A specialized company was then contacted in order to make the remaining parts. Less than one week later, the parts were finished. The other relevant situation was related to the ordering of electronic material in January and February which was delayed several weeks due to bureaucratic issues. Thus, the development of the mechanical and hardware systems was severely affected. Other difficulties were related with finding suitable places to execute ground and flight tests. An urban area such as the region of Porto lacks of wide and unobstructed spaces adequate to perform these experiments. It restrained the amount and the flying time of the tests, since the need of looking for locations outside Porto leaded to a waste of time in travels. Besides that, even the tests conducted at the faculty were always subject to the weather conditions such as wind and rain.

6.2 Conclusions

Controlling a paraglider is not a trivial problem. The pendulum effect along with a non rigid wing structure subjected to the wind influence, make this problem highly challenging. After the study here developed, it was possible to create a device capable of controlling a paraglider. It is able to perform navigation and guidance tasks, leading the STRAPLEX platform to a given location. Drone is intended to be an innovation work not only in the STRAPLEX project, but also in the recoverable stratospheric platforms area. In fact, this module makes the recover operations more reliable and safe.

During the development a series of tests were conducted to evaluate the functionality of each system. This process included ground, low and medium altitude tests reaching a total of more than forty experiments. The first flights, in manual mode, showed a very maneuverable and responsive system. The last ones, at Serra da Freita, allowed longer flights and a bigger confidence in the autonomous modes. Although these flights had not reached the destination, the system tried incessantly counteract the wind effects. Despite the fact that more and longer flights are needed, the preliminary results point to an adequate control algorithm. More tests not only provide enough data to validate the autonomous mode, but will also be used to build a model capable of refining the control algorithm. The 3 m^2 canopy allowed up to 2.8:1 of glide ratio during the tests but a better glide ratio may be achieved with a proper canopy for this application.

The material used as cover proved, again, to be a very effective shock absorbent. Although moderate damages were observed in the Drone capsule after fifteen flights, they were easily repaired with an adhesive agent. These damages, mostly in the bottom area, occurred due to several hard landings. However, as expected, the energy dissipation in the low cost and easy to replace foam, prevented electronic and mechanical failures. After the thirty-third flight, the first malfunction affected the electronic systems. After some analysis it was concluded that a fragile spot in the GPS antenna along with a short clearance between this component and the styrofoam cover, made this device prone to get damaged during the landings. On the other hand, the mechanical actuators setup showed to be an excellent solution since they never got jammed. Indeed, since the assembly, the mechanical system never needed any kind of repairing or tuning intervention. The detailed design work employed in this section paid off in what concerns on the reliability of this system.

The communication systems performed well enabling the exchange of data and the execution of commands. The GFSK bidirectional channel was extensively used during the development and proved to be a very reliable method. The pair GPS receiver and helix active antenna showed a high sensitivity and a short time to first fix. In spite of booting correctly, the SD card loses its file attribution table some minutes later. Since the flight data may be recorded at the STX center software, the time was prioritized to the development of other essential modules. The STX center played a key role during the tests. Tasks such as monitor the GPS, battery or temperature status as well as setup the autonomous modes, were very simple to execute using this software.

The option of using three separate microcontrollers for the Modemrouter showed to be beneficial. A good processing capacity combined with low power consumption allowed an easier programming process. The parallel processing enables a more fluid handling of the different tasks.

The developed cutdown system proved to be effective and safe. Besides a more controllable actuation, the mechanism can be tested and re-armed in less than 30 seconds. This was not possible in previous system that involved burning a cable with a permanent effect.

Although the several adversities this project suffered, the system was successfully built and tested. The experiments showed that in general the subsystems worked as expected and Drone is capable of controlling the canopy. As an experimental approach to the presented problem, it proved to be a reasonable solution with several aspects to be explored. The main objectives were

accomplished but further enhancements are required to be implemented in order to increase the robustness in all environmental conditions.

6.3 Future work

STRAPLEX is an always on development project and the work presented here is the basis for further enhancements. This contribution aims to be a step to maintain this project in the leading edge of small sized stratospheric platforms.

Since the beginning of this work the canopy has been one of the major concerns. In several flights it was found that with winds stronger than 10 knots, there is no chance of forward progression. A power kite is designed exactly to generate a strong drag comparatively with paragliding canopies. An adequate wing for this application could not only increase the gliding capabilities but also its stability and maneuverability. The landing precision and the chances of returning to the launch point are strongly correlated with these aspects. An enhanced capability of flying into the wind could be achieved by using what is known in paragliding as a speed bar. This technique involves pulling the lines in the front edge of the wing. This lowers the angle of attack and increases the flight speed. Since the breaks are being used only in common mode, they could be connected to only one servo-motor while the remaining one would actuate as a speed bar. Further improvements can be made by joining the main capsule and Drone. This reduces the pendulum effect, the total weight and increases the robustness of the platform. A better landing precision may be possible introducing a small propulsion system to provide a way to progress against the wind in the last minutes before landing.

From the control algorithm point of view, several aspects may be explored. For example, an algorithm capable of adjusting the internal control coefficients based on features like platform mass and canopy size. In what concerns to the navigation, a more robust control may be achieved by using heading and course together instead as separate references. However, to have an accurate heading estimation, a new firmware needs to be flashed to the AHRS unit since the actual version does not enable the gyro temperature compensation. The work developed here is the basis to develop to other layers of autonomy. In this phase, the autopilot consists in following a path determined by localizers or a certain direction. A high level of autonomy could be a path computing with a given landing site in mind **??**. The landing site would be chosen from a database depending on certain aspects such as accessibility, terrain slope and wind direction.

Since the extreme conditions felt at that the stratosphere may affect a variable that is not excited at lower altitudes, a full stratospheric flight must be conducted in order to fully validate this system. This is the next step for the STRAPLEX project.

References

[1] James E. Murray Alex G. Sim and David C. Newfeld. The development and flight test of a deployable precision landing system for spacecraft recovery. Technical report, NASA, September 1993.

[2] David C. Neufeld Patrick K. Rennich Stephen R. Norris James E. Murray, Alex G. Sim and Wesley S. Hughes. Further development and flight test of an autonomous precision landing system using a parafoil. Technical report, NASA, July 1994.

[3] Marilena Vendittelli Chiara Toglia and Leonardo Lanari. Path following for an autonomous paraglider. *49th IEEE Conference on Decision and Control*, pages 4869–4874, December 2010.

[4] Oleg A. Yakimenko Nathan J. Slegers. Optimal control for terminal guidance of autonomous parafoils. AIAA Aerodynamic Decelarator Sytems Technology Conference and Seminar, May 2009.

[5] Chiara Toglia and Marilena Vendittelli. Modeling and motion analysis of autonomous paragliders. Technical report, Università di Roma "La Sapienza".

[6] Isaac I. Kaminer and Oleg A. Yakimenko. Development of control algorithm for the autonomous gliding delivery system. AIAA Aerodynamic Decelarator Sytems Technology Conference and Seminar, May 2003.

[7] Masahito Watanabe and Yoshimasa Ochi. Modeling and motion analysis for a powered paraglider. SICE Annual Conference 2007, September 2007.

[8] Justin Barber Jean-Christophe Berland and Bill Gargano. Autonomous precision delivery of 42,000 pounds under one parachute. AIAA Aerodynamic Decelarator Sytems Technology Conference and Seminar, May 2009.

[9] Eugene A. Bourakov Charles W. Hewgley Alex B. Bordetsky Red P. Jensen Andrew B. Robinson Josh R. Malone Oleg A. Yakimenko, Nathan J. Sledgers and Phil E. Heidt. Mobile system for precise aero delivery with global reach network capability. IEEE International Conference on Control and Automation, December 2009.

[10] David Erdos and Steve E. Watkins. Uav autopilot integration and testing.

[11] Jianwu Zheng Zhiqiang Sun, Zhiyoung Li. Influence of improper installation on measurement performance of a pitot tube. International Conference on Industrial Mechatronics and Automation, 2009.

[12] Robert M. Rogers. Aerodynamic parameter estimation for controlled parachutes. AIAA Atmospheric flight mechanics conference and exhibit, 2002.